Mechanics of Materials 202 (2025) 105215

Contents lists available at ScienceDirect

Mechanics of Materials

journal homepage: www.elsevier.com/locate/mecmat

Research paper

Homogenised modelling of the electro-mechanical behaviour of a vascularised poroelastic composite representing the myocardium

Laura Miller [a,b], Raimondo Penta [a,*]

[a] School of Mathematics and Statistics, University of Glasgow, University Place, Glasgow, G12 8QQ, UK
[b] Department of Mathematics and Statistics, University of Strathclyde, 26 Richmond Street, Glasgow, G1 1XH, UK

ARTICLE INFO

Keywords:
Poroelasticity
Asymptotic homogenisation
Myocardial modelling
Vascularisation

ABSTRACT

We propose a novel model for a vascularised poroelastic composite representing the myocardium which incorporates both mechanical deformations and electrical conductivity. Our structure comprises a vascularised poroelastic extracellular matrix with an embedded elastic inclusions (representing the myocytes) and we consider the electrical conductance between these two solid compartments. There is a distinct lengthscale separation between the scale where we can visibly see the connected fluid compartment separated from the poroelastic matrix and the elastic myocyte and the overall size of the heart muscle. We therefore apply the asymptotic homogenisation technique to derive the new model. The effective governing equations that we obtain describe the behaviour of the myocardium in terms of the zero-th order stresses, current densities, relative fluid–solid velocities, pressures, electric potentials and elastic displacements. It effectively accounts for the fluid filling in the pores of the poroelastic matrix, flow in the vessels, the transport of fluid between the vessels and the matrix, and the elastic deformation and electrical conductance between the poroelastic matrix and the myocyte. This work paves the way towards a myocardium model that incorporates multiscale deformations and electrical conductivity whilst also considering the effects of the vascularisation and indeed the impact on mechanotransduction.

1. Introduction

The human heart pumps blood around the body using the strength of its muscular walls which possess a layered microstructure. The three distinct layers are the endocardium, the myocardium, and the epicardium. The myocardium is the most dominant layer and is found between the thin epicardium and endocardium. As the myocardium is the most dominant layer it has its own blood supply via the coronary arteries. The myocardium is susceptible to a variety of diseases, such as myocardial infarction, angina and the effects of ageing (Whitaker, 2014; Weinhaus and Roberts, 2005).

The myocardium of the heart is formed from individual cardiac muscle cells, which are called myocytes. The myocytes are connected end to end at the gap junctions by the intercalated discs. This means that between adjacent myocytes there exist strong electrical and mechanical connections in every direction. This allows the myocardium to act as a single contractile unit (Bader et al., 2021) with fast and coordinated contraction throughout. The electrical activation creates the contraction of the heart muscle which then pumps blood around the body. The electrophysiology of the heart is complex and has many features that should be taken into account such as ion channels and the transport of ions, for further details on cardiac electrophysiology the reader is directed to Katz (2010), Opie (2004) and Weidmann (1974).

The myocardium has a microstructure where we can identify cardiac myocytes surrounded by a collagen matrix (which is produced by the cardiac fibroblasts) with an interconnected blood flow through the permeating vasculature (Purslow, 2008). We can only identify these structures on a microscale length which is much smaller than the size of the entire heart muscle. The microstructure of the myocardium is very complex geometrically and for this reason is strongly impacted by a variety of diseases, in particular myocardial infarction. In the case of myocardial infarction we have a reduction in the blood flow and therefore the myocytes do not receive enough oxygen and nutrients and therefore cannot survive. In their place the fibroblasts create a collagen rich scar tissue to retain the structural integrity of the heart.

Due to the heart being a very complex organ both structurally and in terms of its behaviours this has mean that it is a key area for investigation by researchers. The electrophysiology, mechanical behaviour and modelling the heart as a porous medium has resulted in a variety of modelling

* Corresponding author.
E-mail address: Raimondo.Penta@glasgow.ac.uk (R. Penta).

https://doi.org/10.1016/j.mechmat.2024.105215
Received 12 September 2024; Received in revised form 22 November 2024; Accepted 27 November 2024
Available online 20 December 2024

approaches (Peirlinck et al., 2021; Owen et al., 2018; Smith et al., 2004; Cookson et al., 2012; Ng et al., 2005; Pesavento et al., 2017; Di Gregorio et al., 2021). An extremely prominent approach is modelling the myocardium via constitutive nonlinear elastic theory via the Holzapfel–Ogden law (Holzapfel and Ogden, 2009). This incorporates the underlying microstructural collagen and elastin fibre orientations when modelling the myocardium as a layered structure.

Since the heart is multiscale in nature, to capture its behaviour correctly, we create computationally feasible models where the macroscale effective governing equations encode the properties and interactions of the microscale constituents. To create such a model we must setup a problem that consists of the governing equations for each microstructural constituent and interface conditions describing the interactions that occur between them. Problems of this kind can be upscaled via a wide range of techniques. The upscaling leads to a macroscale system of effective governing equations. These upscaling methods are known as homogenisation techniques and have been described in detail in Hori and Nemat-Nasser (1999) and Davit et al. (2013). Some examples of homogenisation techniques are mixture theory, effective medium theory, volume averaging, and asymptotic homogenisation. Each of these methods has advantages and disadvantages and the choice of technique should be made by considering the desired characteristics of the macroscale model.

In this case we choose to apply the asymptotic homogenisation technique, which has been utilised by many works in the literature. It has been popularly used in the theory of poroelasticity such as in Burridge and Keller (1981) and Penta et al. (2020), in the modelling of elastic materials with composite microstructures (Penta and Gerisch, 2015, 2017a), and also applied to materials that are electroactive in Di Stefano et al. (2020), Penta et al. (2018) and Penta et al. (2021). The technique has been very important in extending the theory of poroelasticity and has been used to include important biological phenomena such as growth and remodelling and vascularisation (Penta et al., 2014; Penta and Merodio, 2017; Mascheroni et al., 2023). The theory of poroelasticity was further extended to include poroelastic materials with more complicated microstructures such as poroelastic composites and double poroelastic materials (Miller and Penta, 2020, 2021a) via the asymptotic homogenisation technique. A major benefit of using the asymptotic homogenisation technique is that the models that arise are computationally feasible. This feature has allowed for computational studies investigating properties of poroelastic materials such as the effective stiffness, porosity and compressibility to be considered in Miller and Penta (2022b) and Dehghani et al. (2018). The technique has also been applied to model double porosity in fluid-saturated elastic media by Rohan et al. (2016). This work takes into consideration the interplay of a poroelastic phase and an interconnected fluid phase. This model was then used for the specific application of compact bone in Rohan et al. (2012). This model has indeed many applications which is further evidenced by the investigations into tissue perfusion carried out in Rohan and Cimrman (2010) and Rohan et al. (2021).

In addition to all these examples, heart modelling has been previously approached via the asymptotic homogenisation technique, for example the structural changes cause as a result of myocardial infarction have been investigated numerically in Miller and Penta (2022a). The electrical bidomain model (Bader et al., 2021; Richardson and Chapman, 2011) has been considered and derived using the asymptotic homogenisation technique, as well as the electrical and mechanical bidomain model of the heart (Miller and Penta, 2023).

In this work we apply the asymptotic homogenisation technique to a problem that we have set up to describe the mechanical and electrical deformations of the perfused myocardium. We assume that the size of the heart is much larger than the scale where we can identify the elastic myocytes, the poroelastic extracellular matrix and the permeating vasculature. We call this scale the microscale. We associate a length with the microscale that is much smaller than the length of the entire heart muscle. If we zoom in further on the extracellular matrix portion of the microscale then we find that the domain is a porous matrix with fluid flowing in the pores. To account for this porescale microstructure we use the governing equations of Biot's poroelasticity for the extracellular matrix. When looking at the entire heart muscle we no longer see the myocytes or the blood vessels as the variations are smoothed out and so we denote the scale of the heart as the macroscale. We are then able to apply the asymptotic homogenisation technique to upscale the problem we have described on the microstructure, by accounting for the continuity of current densities, stresses, elastic displacements, and then also the difference in the electric potentials and by accounting for the zero flux across the interface between the elastic myocyte and the poroelastic extracellular matrix and by accounting for the continuity of fluxes, stresses, fluid transport, slip over the porous surface, and the insulation of the current density on the interface between the vascular network and the poroelastic extracellular matrix.

The novel macroscale PDEs model that is derived contains a balance equation for the current densities and a balance equation for the stresses. These balance equations contain additional terms that allow for the model to account for the difference in the electric potentials at different points in the microstructure. The model also comprises two balance equations of the relative fluid–solid velocities of the vessels and interstitial fluid. These contain terms related to the strains of the elastic myocyte and the poroelastic extracellular matrix and to the fluid transport between the compartments due to the leakage of the fluid from the vessels into the poroelastic matrix. The macroscale model coefficients allow for the properties of the microstructure to be retained in the macroscale model and these are to be computed by solving the microscale differential problems of the asymptotic homogenisation technique.

The current work builds upon prominent modelling approaches in the literature such as the model for vascularised poroelastic materials by Penta and Merodio (2017), the electrical and mechanical bidomain model of Miller and Penta (2023) and the models of a poroelastic matrix with elastic inclusion by Royer et al. (2019) and Chen et al. (2020). This work combines key features from Penta and Merodio (2017) and Miller and Penta (2023) to create a vascularised, electrical and mechanical myocardium model. The model will encode structural and behavioural features of the myocardium over two distinct finer scales. This level of microstructural detail being encoded in the final macroscale model allows for a greater understanding of the myocardial behaviour due to a more realistic microstructure being considered. Our model captures elastic behaviour, electrical activity and perfusion and therefore paves the way towards a computationally feasible microstructurally motivated myocardium model which can be used to understand whether the differences in myocyte and extracellular matrix displacements and perfusion effects the mechanotransduction of the overall heart and hence greater understanding of the influence of disease.

We structure the remainder of this work as follows. In Section 2 we introduce the governing equations for each phase in our microstructure that describes the myocardium. Then in Section 3 we carry out a multiple scales expansion and apply the asymptotic homogenisation technique to derive the equations governing the myocardium in terms of the zero-th order quantities. The macroscale results are presented in Section 4. We then provide a numerical example investigating the electrical conductivity of the perfused myocardium in Section 5. Finally we provide a summary of our work and future perspectives in Section 6. We additionally have an Appendix that comprises a scheme that can be utilised to solve the macroscale model.

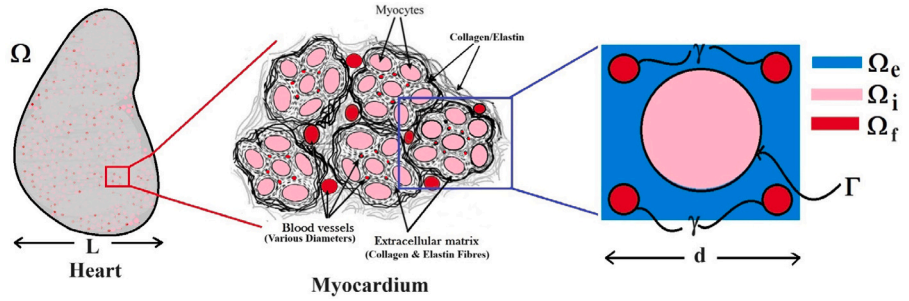

Fig. 1. A 2D sketch representing the multiple scales in the myocardium. The myocyte Ω_i is shown in pink and the extracellular domain Ω_e is in blue. There is an interface Γ between the two domains. There is also the fluid compartment shown in red which is in contact with just the extracellular domain via the interface γ.

2. Problem

We wish to study the microstructure of the myocardium which we define as a set $\Omega \in \mathbb{R}^3$ with Ω as the union of the extracellular matrix Ω_e, the myocyte Ω_i, and an interconnected vascular fluid network Ω_f with $\bar{\Omega} = \bar{\Omega}_i \cup \bar{\Omega}_e \cup \bar{\Omega}_\mathrm{f}$. A sketch of a cross-section of our domain Ω is given in Fig. 1.

We now introduce the equations that we will use to describe each domain, as well as appropriate interface conditions that will close the problem. To describe the electrical conductivity in each domain we use the passive steady-state electrical bidomain equations, as introduced in Roth (1991, 1992, 2016). We have

$$\nabla \cdot (\mathsf{G}_i \nabla \phi_i) = \beta G(\phi_i - \phi_e) - I_i \quad \text{in} \quad \Omega_i, \tag{1a}$$

$$\nabla \cdot (\mathsf{G}_e \nabla \phi_e) = -\beta G(\phi_i - \phi_e) - I_e \quad \text{in} \quad \Omega_e, \tag{1b}$$

where we have that G_i and G_e are the second rank conductivity tensors in the myocyte and extracellular matrix respectively, the scalar electric potentials in each domain are given by ϕ_i and ϕ_e, the scalars β and G are the ratio of membrane area to tissue volume and membrane conductance parameters respectively, and I_i and I_e are source terms in the myocyte and extracellular matrix respectively. We note that in following Roth (1992) we also assume that at any point within the tissue, the difference between the myocyte and extracellular potentials is equal to the transmembrane potential which we call V and will appear in equations to follow. These steady-state bidomain Eqs. (1a) and (1b) are written in terms of the balance of the electric current density in each domain, which we can write as

$$\mathbf{j}_i = -\mathsf{G}_i \nabla \phi_i \quad \text{in} \quad \Omega_i, \tag{2a}$$

$$\mathbf{j}_e = -\mathsf{G}_e \nabla \phi_e \quad \text{in} \quad \Omega_e. \tag{2b}$$

These are given by Ohm's Law with conductivity tensors G_i and G_e and we write the applied electric fields as $\nabla\phi_i$ and $\nabla\phi_e$.

We now require the mechanical equations in each domain. We have the following balance equations

$$\nabla \cdot \mathsf{T}_i = -\mathsf{G}_i \nabla \phi_i \times \mathbf{B} \quad \text{in} \quad \Omega_i, \tag{3a}$$

$$\nabla \cdot \mathsf{T}_e = -\mathsf{G}_e \nabla \phi_e \times \mathbf{B} \quad \text{in} \quad \Omega_e, \tag{3b}$$

where T_i is the stress tensor in the myocyte and T_e is the effective stress tensor in the extracellular matrix, $\mathbf{u}_i$ and $\mathbf{u}_e$ are the elastic displacements in the myocyte and matrix respectively. We see from the balance Eqs. (3a) and (3b) that each domain is subject to a body force. This is a Lorentz force on the action potential currents, $\mathbf{j}_i$ and $\mathbf{j}_e$, where we have a magnetic field $\mathbf{B}$ (Puwal and Roth, 2010). We can write these body forces as

$$\mathbf{j}_i \times \mathbf{B} = -\mathsf{G}_i \nabla \phi_i \times \mathbf{B} \quad \text{and} \quad \mathbf{j}_e \times \mathbf{B} = -\mathsf{G}_e \nabla \phi_e \times \mathbf{B}. \tag{4}$$

The body forces used here were chosen for a variety of reasons. The initial reason being this force has been previously considered in Puwal and Roth (2010) when creating a mechanical bidomain model and investigating the effect of magnetic forces on action currents associated with a propagating action potential wave front. By using also this force we will be able to compare with the numerical results obtained by Puwal and Roth (2010). The second reason for this choice of body force is that there are important applications where the Lorentz force has been used in imaging, e.g. elastic displacement due to Lorentz force has been recently proposed as a potential use of MRI . We direct the reader to Dorfmann and Ogden (2006, 2014), Maugin (2013), Fu (2024) and Liguori and Gei (2023) for further details on electroelastic materials and the effects of applied electric body forces.

We assume that the myocyte is an anisotropic linear elastic material and therefore has a stress tensor which can be written as

$$\mathsf{T}_i = \mathbb{C}_i \nabla \mathbf{u}_i \quad \text{in} \quad \Omega_i, \tag{5}$$

where $\mathbb{C}_i$ is the fourth rank elasticity tensor with corresponding components $(C^i)_{\alpha\delta\tau\kappa}$, for $\alpha, \delta, \tau, \kappa = 1, 2, 3$, and $\mathbf{u}_i$ is the elastic displacement in the myocyte. We assume that the extracellular matrix is a poroelastic material with the effective stress tensor

$$\mathsf{T}_e = \mathbb{C}_e \nabla \mathbf{u}_e - \hat{\boldsymbol{\alpha}}_e p_p \quad \text{in} \quad \Omega_e, \tag{6}$$

where $\mathbb{C}_e$ is the fourth rank effective elasticity tensor with corresponding components $(C^e)_{\alpha\delta\tau\kappa}$, for $\alpha, \delta, \tau, \kappa = 1, 2, 3$, $\mathbf{u}_e$ is the elastic displacement $\hat{\boldsymbol{\alpha}}_e$ is the Biot's tensor of coefficients and p_p is the interstitial pressure of the fluid in the pores. The coefficients $\mathbb{C}_e$ and $\hat{\boldsymbol{\alpha}}_e$ can be obtained via a finer scale homogenisation process such as those detailed in Burridge and Keller (1981) and Penta et al. (2020).

We have that the tensors $\mathbb{C}_i$ and $\mathbb{C}_e$ are equipped with right minor and major symmetries, these are defined as

$$(C^i)_{\alpha\delta\tau\kappa} = (C^i)_{\alpha\delta\kappa\tau}; \quad (C^e)_{\alpha\delta\tau\kappa} = (C^e)_{\alpha\delta\kappa\tau}, \tag{7a}$$

$$(C^i)_{\alpha\delta\tau\kappa} = (C^i)_{\tau\kappa\alpha\delta}; \quad (C^e)_{\alpha\delta\tau\kappa} = (C^e)_{\tau\kappa\alpha\delta}. \tag{7b}$$

By combining (7a)–(7b) then the left minor symmetries follow. By using the right minor symmetries we can rewrite the stress Eqs. (5) and (6) as

$$\mathsf{T}_i = \mathbb{C}_i \xi(\mathbf{u}_i) \qquad \text{in} \quad \Omega_i, \tag{8a}$$

$$\mathsf{T}_e = \mathbb{C}_e \xi(\mathbf{u}_e) - \hat{\boldsymbol{\alpha}}_e p_p \qquad \text{in} \quad \Omega_e, \tag{8b}$$

where we have that

$$\xi(\bullet) = \frac{\nabla(\bullet) + (\nabla(\bullet))^{\mathrm{T}}}{2}, \tag{9}$$

is the symmetric part of the gradient operator.

Since the extracellular matrix is poroelastic we have Darcy's law

$$\mathbf{w}_e = -\mathsf{K}_e \nabla p_p \qquad \text{in} \quad \Omega_e, \tag{10}$$

with the pressure in the pores p_p, hydraulic conductivity tensor K_e and where we have defined using the relative fluid–solid velocity

$$\mathbf{w}_e = \phi(\mathbf{v} - \dot{\mathbf{u}}_e) \qquad \text{in} \quad \Omega_e, \tag{11}$$

where the interstitial fluid velocity is $\mathbf{v}$ and ϕ is the underlying porosity of the poroelastic extracellular matrix.

To completely govern the extracellular matrix portion of our microstructure we have the standard Biot's conservation of mass equation (Biot, 1955, 1956a,b, 1962), which reads

$$\frac{\dot{p_p}}{M} = -\hat{\boldsymbol{\alpha}}_e : \xi(\dot{\mathbf{u}}_e) - \nabla \cdot \mathbf{w}_e \qquad \text{in} \quad \Omega_e, \tag{12}$$

where M is the Biot's modulus and the other terms are defined previously. We should note that the equations we have chosen to govern the extracellular matrix are the equations of Biot's poroelasticity (Biot, 1955, 1956a,b, 1962) which can also be derived via application of the asymptotic homogenisation technique to a finer scale problem that what we are considering here, see Burridge and Keller (1981) and Penta et al. (2020)

Now we consider the fluid in the blood vessels. We require a balance equation for this domain. This is given as

$$\nabla \cdot \mathsf{T}_{\mathrm{f}} = 0 \quad \text{in} \quad \Omega_{\mathrm{f}}, \tag{13}$$

and we have that T_{f} is the fluid stress tensor. We are making the assumption that our fluid is incompressible and Newtonian, and so therefore has the constitutive equation

$$\mathsf{T}_{\mathrm{f}} = -p_{\mathrm{f}} \mathrm{I} + 2\mu \xi(\mathbf{v}_{\mathrm{f}}), \tag{14}$$

where we have $\mathbf{v}_{\mathrm{f}}$ as the fluid velocity, p_{f} is the pressure and μ the viscosity of the fluid. Since the fluid is incompressible we require the incompressibility constraint

$$\nabla \cdot \mathbf{v}_{\mathrm{f}} = 0 \quad \text{in} \quad \Omega_{\mathrm{f}}. \tag{15}$$

By using the constitutive law (14) in the balance Eq. (13) with the incompressibility constraint (15) we obtain the Stokes' problem

$$\mu \nabla^2 \mathbf{v}_{\mathrm{f}} = \nabla p_{\mathrm{f}} \quad \text{in} \quad \Omega_{\mathrm{f}}. \tag{16}$$

We have now described the equations governing each of the subdomains (Ω_i, Ω_e and Ω_{f}). In order to close our problem we require to place conditions on each of the interfaces. We have the interface between the poroelastic matrix and the elastic myocyte which we shall call Γ. We can define this as $\Gamma := \partial\Omega_i \cap \partial\Omega_e$. We also have a second interface between the poroelastic matrix and the embedded fluid phase which we shall call γ. We can define this as $\gamma := \partial\Omega_e \cap \partial\Omega_{\mathrm{f}}$.

First we close the problem by prescribing conditions on the solid–solid interface Γ, these are continuity of the current densities, prescribed jump in electric potential, continuity of stresses, continuity of elastic displacements and the insulation of the fluid flux across the boundary between the poroelastic extracellular matrix and the solid elastic myocyte

$$\mathsf{G}_i \nabla \phi_i \cdot \mathbf{n}_\Gamma = \mathsf{G}_e \nabla \phi_e \cdot \mathbf{n}_\Gamma \qquad \text{on} \quad \Gamma, \tag{17a}$$

$$\phi_i - \phi_e = V \qquad \text{on} \quad \Gamma, \tag{17b}$$

$$\mathsf{T}_i \cdot \mathbf{n}_\Gamma = \mathsf{T}_e \cdot \mathbf{n}_\Gamma \qquad \text{on} \quad \Gamma, \tag{17c}$$

$$\mathbf{u}_i = \mathbf{u}_e \qquad \text{on} \quad \Gamma, \tag{17d}$$

$$\mathbf{w}_e \cdot \mathbf{n}_\Gamma = 0 \qquad \text{on} \quad \Gamma, \tag{17e}$$

where V is a given and is the potential drop across the membrane (Richardson and Chapman, 2011) and $\mathbf{n}_\Gamma$ is the normal to the interface Γ pointing into the myocyte.

We now state the conditions on the interface γ between the blood vessels and the extracellular matrix. These include the continuity of fluxes, continuity of stresses, fluid flow across the interface between the vessels and the extracellular matrix, the fluid slip over a porous surface using the Beavers–Joseph–Saffman condition, and the insulation of the current density from the fluid. We have

$$\mathbf{w}_e \cdot \mathbf{n}_\gamma = \mathbf{w}_{\mathrm{f}} \cdot \mathbf{n}_\gamma \quad \text{on} \quad \gamma, \tag{18a}$$

$$\mathsf{T}_{\mathrm{f}} \mathbf{n}_\gamma = \mathsf{T}_e \mathbf{n}_\gamma \quad \text{on} \quad \gamma, \tag{18b}$$

$$\mathbf{n}_\gamma \cdot (\mathsf{T}_{\mathrm{f}} \mathbf{n}_\gamma) + \frac{1}{L_p}(\mathbf{v}_{\mathrm{f}} - \dot{\mathbf{u}}_e) \cdot \mathbf{n}_\gamma = -p_p \quad \text{on} \quad \gamma, \tag{18c}$$

$$\tau_\beta \cdot (\mathsf{T}_\mathrm{f}\mathbf{n}_\gamma) = -\frac{\alpha}{\sqrt{k}}(\mathbf{v}_\mathrm{f} - \dot{\mathbf{u}}_e)\cdot\tau_\beta \quad \text{on} \quad \gamma, \tag{18d}$$

$$\mathsf{G}_e\nabla\phi_e \cdot \mathbf{n}_\gamma = 0 \quad \text{on} \quad \gamma, \tag{18e}$$

where we have that L_p is the leakage from the vessels, k is the permeability and α is a dimensionless parameter depending on the properties of the interface γ. We have defined $\mathbf{n}_\gamma$ as the normal to the interface γ pointing into the fluid. We note that for the sake of simplicity we are assuming that the electrical current density does not travel into the vessel fluid however this can indeed be modified and extended, see Conclusions Section 6 for further discussion surrounding this extension.

Now that we have described all the equations in our fluid–structure interaction problem we can summarise them here for convenience with their corresponding subdomain or interface included. We have

$$\nabla\cdot(\mathsf{G}_i\nabla\phi_i) = \beta(\phi_i - \phi_e) - I_i \quad \text{in} \quad \Omega_i, \tag{19a}$$

$$\nabla\cdot(\mathsf{G}_e\nabla\phi_e) = -\beta(\phi_i - \phi_e) - I_e \quad \text{in} \quad \Omega_e, \tag{19b}$$

$$\mathbf{j}_i = -\mathsf{G}_i\nabla\phi_i \quad \text{in} \quad \Omega_i, \tag{19c}$$

$$\mathbf{j}_e = -\mathsf{G}_e\nabla\phi_e \quad \text{in} \quad \Omega_e, \tag{19d}$$

$$\nabla\cdot\mathsf{T}_i = -\mathsf{G}_i\nabla\phi_i\times\mathbf{B} \quad \text{in} \quad \Omega_i, \tag{19e}$$

$$\nabla\cdot\mathsf{T}_e = -\mathsf{G}_e\nabla\phi_e\times\mathbf{B} \quad \text{in} \quad \Omega_e, \tag{19f}$$

$$\mathsf{T}_i = \mathbb{C}_i\xi(\mathbf{u}_i) \quad \text{in} \quad \Omega_i, \tag{19g}$$

$$\mathsf{T}_e = \mathbb{C}_e\xi(\mathbf{u}_e) - \hat{\boldsymbol{\alpha}}_e p_p \quad \text{in} \quad \Omega_e, \tag{19h}$$

$$\mathbf{w}_e = -\mathsf{K}_e\nabla p_p \quad \text{in} \quad \Omega_e, \tag{19i}$$

$$\frac{\dot{p_p}}{M} = -\hat{\boldsymbol{\alpha}}_e : \xi(\dot{\mathbf{u}}_e) - \nabla\cdot\mathbf{w}_e \quad \text{in} \quad \Omega_e, \tag{19j}$$

$$\nabla\cdot\mathsf{T}_\mathrm{f} = 0 \quad \text{in} \quad \Omega_\mathrm{f}, \tag{19k}$$

$$\mathsf{T}_\mathrm{f} = -p_\mathrm{f}\mathrm{I} + 2\mu\xi(\mathbf{v}_\mathrm{f}) \quad \text{in} \quad \Omega_\mathrm{f}, \tag{19l}$$

$$\nabla\cdot\mathbf{v}_\mathrm{f} = 0 \quad \text{in} \quad \Omega_\mathrm{f} \tag{19m}$$

$$\mu\nabla^2\mathbf{v}_\mathrm{f} = \nabla p_\mathrm{f} \quad \text{in} \quad \Omega_\mathrm{f} \tag{19n}$$

$$\mathsf{T}_i\cdot\mathbf{n}_\Gamma = \mathsf{T}_e\cdot\mathbf{n}_\Gamma \quad \text{on} \quad \Gamma, \tag{19o}$$

$$\mathbf{u}_i = \mathbf{u}_e \quad \text{on} \quad \Gamma, \tag{19p}$$

$$\mathsf{G}_i\nabla\phi_i\cdot\mathbf{n}_\Gamma = \mathsf{G}_e\nabla\phi_e\cdot\mathbf{n}_\Gamma \quad \text{on} \quad \Gamma, \tag{19q}$$

$$\phi_i - \phi_e = V \quad \text{on} \quad \Gamma, \tag{19r}$$

$$\mathbf{w}_e\cdot\mathbf{n}_\Gamma = 0 \quad \text{on} \quad \Gamma, \tag{19s}$$

$$\mathbf{w}_e\cdot\mathbf{n}_\gamma = \mathbf{w}_\mathrm{f}\cdot\mathbf{n}_\gamma \quad \text{on} \quad \gamma, \tag{19t}$$

$$\mathsf{T}_\mathrm{f}\mathbf{n}_\gamma = \mathsf{T}_e\mathbf{n}_\gamma \quad \text{on} \quad \gamma, \tag{19u}$$

$$\mathbf{n}_\gamma\cdot(\mathsf{T}_\mathrm{f}\mathbf{n}_\gamma) + \frac{1}{L_p}(\mathbf{v}_\mathrm{f} - \dot{\mathbf{u}}_e)\cdot\mathbf{n}_\gamma = -p_p \quad \text{on} \quad \gamma, \tag{19v}$$

$$\tau_\beta\cdot(\mathsf{T}_\mathrm{f}\mathbf{n}_\gamma) = -\frac{\alpha}{\sqrt{k}}(\mathbf{v}_\mathrm{f} - \dot{\mathbf{u}}_e)\cdot\tau_\beta \quad \text{on} \quad \gamma, \tag{19w}$$

$$\mathsf{G}_e\nabla\phi_e\cdot\mathbf{n}_\gamma = 0 \quad \text{on} \quad \gamma. \tag{19x}$$

To begin the derivation of our model we must perform a multiscale analysis. To do this we begin by (i) non-dimensionalising the problem that we have just introduced in this section, then (ii) introduce two well-separated length scales, (iii) we then apply the two scale asymptotic homogenisation technique to the non-dimensional equations that govern each domain, and (iv) determine the macroscale equations describing the effective behaviour of the myocardium.

3. Multiscale analysis

The heart can be characterised by two different length scales, see Fig. 1. We associate the average lengthscale of the heart by L (the macroscale), and we have a second lengthscale d which we call the microscale, and we assume that this is comparable with the distance between adjacent myocytes and vessels. To emphasise the difference between the two scales, we perform a non-dimensional analysis of the problem presented in Section 2.

3.1. Non–dimensionalisation of the problem

We wish to understand the mutual weights of each of the relevant fields in the problem and therefore we formulate the model in non–dimensional form. This means that we will capture the correct asymptotic behaviour of the material once we apply the asymptotic homogenisation technique. The model that we will derive is assumed to describe the myocardium in a healthy scenario but will allow for modifications to certain conditions or diseases at a further stage. Due to the desire to keep the model as general as possible we do not choose specific condition or disease related

parameters to carry out the non–dimensionalisation. We do however perform a formal non–dimensionalisation that indicates the appropriate asymptotic behaviour of each of the relevant fields.

We choose to scale the spatial variable and the elastic displacement by the characteristic length scale L of the heart muscle. This means that the stresses and elasticity tensors will also be scaled by L. We make the assumption that the system can be characterised by a reference pressure gradient C, and that the characteristic fluid velocity is given by the typical parabolic profile proportional to that of a Newtonian fluid slowly flowing in a cylinder of radius d. We choose that the change in electric potential can be scaled by Φ_0 and the electrical conductivities are scaled by G_0, the typical conductance. We therefore non–dimensionalise by using

$$\begin{gathered}\mathbf{x} = L\mathbf{x}', \quad \mathbb{C}_i = CL\mathbb{C}_i', \quad \mathbb{C}_e = CL\mathbb{C}_e', \quad \mathsf{T}_i = CL\mathsf{T}_i', \quad \mathsf{T}_e = CL\mathsf{T}_e', \quad \mathbf{u}_e = L\mathbf{u}_e', \\ \mathbf{u}_i = L\mathbf{u}_i', \quad \phi_i = \Phi_0\phi_i', \quad \phi_e = \Phi_0\phi_e', \quad V = \Phi_0 V', \quad \mathsf{G}_i = \mathsf{G}_0\mathsf{G}_i', \\ \mathsf{G}_e = \mathsf{G}_0\mathsf{G}_e', \quad \mathbf{B} = \frac{L}{\mathsf{G}_0\Phi_0}\mathbf{B}', \quad \mathbf{v} = \frac{Cd^2}{\mu}\mathbf{v}', \quad p = CLp'.\end{gathered} \tag{20}$$

We note that the gradient operator can be scaled as

$$\nabla = \frac{1}{L}\nabla'. \tag{21}$$

We now use these scalings and obtain the non-dimensionalised form of the microscale governing equations

$$\nabla\cdot(\mathsf{G}_i\nabla\phi_i) = \hat{\beta}(\phi_i - \phi_e) - I_i \quad \text{in} \quad \Omega_i, \tag{22a}$$

$$\nabla\cdot(\mathsf{G}_e\nabla\phi_e) = -\hat{\beta}(\phi_i - \phi_e) - I_e \quad \text{in} \quad \Omega_e, \tag{22b}$$

$$\mathbf{j}_i = -\mathsf{G}_i\nabla\phi_i \quad \text{in} \quad \Omega_i, \tag{22c}$$

$$\mathbf{j}_e = -\mathsf{G}_e\nabla\phi_e \quad \text{in} \quad \Omega_e, \tag{22d}$$

$$\nabla\cdot\mathsf{T}_i = -\mathsf{G}_i\nabla\phi_i\times\mathbf{B} \quad \text{in} \quad \Omega_i, \tag{22e}$$

$$\nabla\cdot\mathsf{T}_e = -\mathsf{G}_e\nabla\phi_e\times\mathbf{B} \quad \text{in} \quad \Omega_e, \tag{22f}$$

$$\mathsf{T}_i = \mathbb{C}_i\xi(\mathbf{u}_i) \quad \text{in} \quad \Omega_i, \tag{22g}$$

$$\mathsf{T}_e = \mathbb{C}_e\xi(\mathbf{u}_e) - \hat{\boldsymbol{\alpha}}_e p_p \quad \text{in} \quad \Omega_e, \tag{22h}$$

$$\mathbf{w}_e = -\mathsf{K}_e\nabla p_p \quad \text{in} \quad \Omega_e, \tag{22i}$$

$$\frac{\dot{p_p}}{M} = -\hat{\boldsymbol{\alpha}}_e : \xi(\dot{\mathbf{u}}_e) - \nabla\cdot\mathbf{w}_e \quad \text{in} \quad \Omega_e, \tag{22j}$$

$$\nabla\cdot\mathsf{T}_\mathrm{f} = 0 \quad \text{in} \quad \Omega_\mathrm{f}, \tag{22k}$$

$$\mathsf{T}_\mathrm{f} = -p_\mathrm{f}\mathbf{I} + \epsilon^2\xi(\mathbf{v}_\mathrm{f}) \quad \text{in} \quad \Omega_\mathrm{f}, \tag{22l}$$

$$\nabla\cdot\mathbf{v}_\mathrm{f} = 0 \quad \text{in} \quad \Omega_\mathrm{f} \tag{22m}$$

$$\epsilon^2\nabla^2\mathbf{v}_\mathrm{f} = \nabla p_\mathrm{f} \quad \text{in} \quad \Omega_\mathrm{f} \tag{22n}$$

$$\mathsf{T}_i\cdot\mathbf{n}_\Gamma = \mathsf{T}_e\cdot\mathbf{n}_\Gamma \quad \text{on} \quad \Gamma, \tag{22o}$$

$$\mathbf{u}_i = \mathbf{u}_e \quad \text{on} \quad \Gamma, \tag{22p}$$

$$\mathsf{G}_i\nabla\phi_i\cdot\mathbf{n}_\Gamma = \mathsf{G}_e\nabla\phi_e\cdot\mathbf{n}_\Gamma \quad \text{on} \quad \Gamma, \tag{22q}$$

$$\phi_i - \phi_e = V \quad \text{on} \quad \Gamma, \tag{22r}$$

$$\mathbf{w}_e\cdot\mathbf{n}_\Gamma = 0 \quad \text{on} \quad \Gamma, \tag{22s}$$

$$\mathbf{w}_e\cdot\mathbf{n}_\gamma = \mathbf{w}_\mathrm{f}\cdot\mathbf{n}_\gamma \quad \text{on} \quad \gamma, \tag{22t}$$

$$\mathsf{T}_\mathrm{f}\mathbf{n}_\gamma = \mathsf{T}_e\mathbf{n}_\gamma \quad \text{on} \quad \gamma, \tag{22u}$$

$$\mathbf{n}_\gamma\cdot(\mathsf{T}_\mathrm{f}\mathbf{n}_\gamma) + \frac{1}{\epsilon L_p}(\mathbf{v}_\mathrm{f} - \dot{\mathbf{u}}_e)\cdot\mathbf{n}_\gamma = -p_p \quad \text{on} \quad \gamma, \tag{22v}$$

$$\tau_\beta\cdot(\mathsf{T}_\mathrm{f}\mathbf{n}_\gamma) = -\epsilon\frac{\alpha}{\sqrt{k}}(\mathbf{v}_\mathrm{f} - \dot{\mathbf{u}}_e)\cdot\tau_\beta \quad \text{on} \quad \gamma, \tag{22w}$$

$$\mathsf{G}_e\nabla\phi_e\cdot\mathbf{n}_\gamma = 0 \quad \text{on} \quad \gamma. \tag{22x}$$

where we can define

$$\epsilon = \frac{d}{L}, \tag{23}$$

and we have that

$$\hat{\beta} = \frac{\beta G L^2}{G_0}, \tag{24}$$

is a dimensionless parameter associated with the ratio between membrane area and tissue volume. We can see that during the non-dimensionalisation Eqs. (22l), (22n), (22v), and (22w) all gain a scaling by a power of epsilon. This will allow us to obtain the correct asymptotic behaviour when applying the upscaling. For example the ϵ^2 scaling which appears in (22l) is the standard scaling for Stokes' flow and represents the asymptotic behaviour of the characteristic fluid velocity flowing in the pores (Sanchez-Palencia, 2006; Penta et al., 2020, 2014).

Now that we have obtained the non-dimensional system of PDEs (22a)–(22x) we can introduce the two scale asymptotic homogenisation technique which will derive the new model by enforcing the assumption that the microscale and the macroscale are well separated.

3.2. The asymptotic homogenisation technique

Here we now introduce the asymptotic homogenisation technique which we will then use to derive a macroscale model describing the perfused electrical myocardium from the Eqs. (22a)–(22x). The first assumption that we make is that the microscale (where individual myocytes and vessels are clearly resolved from the extracellular matrix), denoted by d, is very small in comparison with average size of the heart muscle L. That is,

$$\epsilon = \frac{d}{L} \ll 1. \tag{25}$$

Since we have two well separated scales we require a local spatial variable that will capture the microscale variations of the fields. We have

$$\mathbf{y} = \frac{\mathbf{x}}{\epsilon}. \tag{26}$$

We note that the spatial variables $\mathbf{x}$ and $\mathbf{y}$ are formally independent and are representative of the macroscale and the microscale, respectively. Due to the two independent scales we must transform the gradient operator

$$\nabla \to \nabla_x + \frac{1}{\epsilon}\nabla_y. \tag{27}$$

We assume that all the fields in our analysis are functions of both variables $\mathbf{x}$ and $\mathbf{y}$. We also assume that the fields can be represented in terms of a power series of ϵ, i.e.

$$\varphi^\epsilon(\mathbf{x},\mathbf{y},t) = \sum_{l=0}^{\infty} \varphi^{(l)}(\mathbf{x},\mathbf{y},t)\epsilon^l, \tag{28}$$

where φ is representative of a typical field involved in our analysis.

In order to allow the analysis to be carried out we make the same assumption as in Richardson and Chapman (2011) and let the electric potential V be a given with the following expansion

$$V = V^{(0)}(\mathbf{x},t) + \cdots, \tag{29}$$

that is, V depends only on the macroscale at order zero.

Before carrying out the analysis we make two more assumptions.

Remark 3.1 (*Microscale Periodicity*)**.** The analysis in this work can be simplified by considering only a single subset of the domain which we denote as a periodic cell. For this to be the case we make the assumption that every field $\varphi^{(l)}$ in (22a)–(22x) is $\mathbf{y}$-periodic. This assumption allows for the microscale differential problems that are a feature of the asymptotic homogenisation technique can be solved on just a finite subset of the material which leads to a reduced computational cost. This assumption is not necessary per se, and the analysis can indeed be carried out by assuming that the fields are only locally bounded. By taking a local boundedness approach we would only determine the functional form of the macroscale model where the coefficients are to be obtained from microscale problems that need to be solved on the whole microstructure of the material. Therefore solving the model derived via local boundedness is very computationally expensive in comparison with microscale periodicity. For further information and examples see Burridge and Keller (1981) and Penta and Gerisch (2017b).

Remark 3.2 (*Macroscopic Uniformity*)**.** In multiscale materials it is well known that at different macroscale points the underlying microstructure can vary. Such a variation has been investigated by Penta et al. (2014), Burridge and Keller (1981), Holmes (2012), Penta and Gerisch (2015) and Dalwadi et al. (2015). By considering that the microscale varies with respect to the macroscale point this requires additional terms in the final model that arise via proper application of the Reynolds transport theorem. This will dramatically increase the computational cost. Therefore here we neglect this dependence to simplify the derivation of the model. We therefore have a material which at every macroscale point possesses the same underlying microstructure. We can equivalently say the microscale geometry does not depend on $\mathbf{x}$. We call this property macroscopic uniformity and we have the simple differentiation under the integral sign

$$\int_\Omega \nabla_{\mathbf{x}} \cdot (\bullet) \mathrm{d}\mathbf{y} = \nabla_x \cdot \int_\Omega (\bullet) \mathrm{d}\mathbf{y}, \tag{30}$$

where $(\bullet)$ is a tensor or a vector quantity.

Remark 3.3 (*Periodic Cell*)**.** Before beginning the analysis we make the identification between the domain Ω and the corresponding periodic cell, where the extracellular matrix, myocyte and fluid vasculature portions are denoted by Ω_e, Ω_i, and Ω_f, respectively. We can identify the interfaces between the different domains as $\Gamma := \partial\Omega_e \cap \partial\Omega_i$, $\gamma := \partial\Omega_e \cap \partial\Omega_\mathrm{f}$. These interfaces have corresponding unit normals $\mathbf{n}_\Gamma$ and $\mathbf{n}_\gamma$. This cell is shown in Fig. 1. We have that $|\Omega| = |\Omega_i| + |\Omega_e| + |\Omega_\mathrm{f}|$ is the domain volume and is equal to 1 since we assume we have a unit cube. Our periodic cell (cube) has periodic boundary conditions applied on all the faces, where we have assumed that the vessels and myocytes extend only in the z-axis direction.

3.3. Multiple scales expansion

We are now ready to begin the derivation of the macroscale model. We can apply the assumptions (27) and (28) of the asymptotic homogenisation technique to the Eqs. (22a)–(22x) to obtain, accounting for periodicity, the following

$$\epsilon^2\nabla_{\mathbf{x}}\cdot(\mathsf{G}_i\nabla_{\mathbf{x}}\phi_i^\epsilon) + \epsilon\nabla_{\mathbf{x}}\cdot(\mathsf{G}_i\nabla_{\mathbf{y}}\phi_i^\epsilon) + \epsilon\nabla_{\mathbf{y}}\cdot(\mathsf{G}_i\nabla_{\mathbf{x}}\phi_i^\epsilon) + \nabla_{\mathbf{y}}\cdot(\mathsf{G}_i\nabla_{\mathbf{y}}\phi_i^\epsilon) = \epsilon^2\hat{\beta}(\phi_i^\epsilon - \phi_e^\epsilon) - \epsilon^2 I_i^\epsilon \quad \text{in} \quad \Omega_i, \tag{31a}$$

$$\epsilon^2\nabla_{\mathbf{x}}\cdot(\mathsf{G}_e\nabla_{\mathbf{x}}\phi_e^\epsilon) + \epsilon\nabla_{\mathbf{x}}\cdot(\mathsf{G}_e\nabla_{\mathbf{y}}\phi_e^\epsilon) + \epsilon\nabla_{\mathbf{y}}\cdot(\mathsf{G}_e\nabla_{\mathbf{x}}\phi_e^\epsilon) + \nabla_{\mathbf{y}}\cdot(\mathsf{G}_e\nabla_{\mathbf{y}}\phi_e^\epsilon) = -\epsilon^2\hat{\beta}(\phi_i^\epsilon - \phi_e^\epsilon) - \epsilon^2 I_e^\epsilon \quad \text{in} \quad \Omega_e, \tag{31b}$$

$$\epsilon\mathbf{j}_i^\epsilon = -\epsilon\mathsf{G}_i\nabla_{\mathbf{x}}\phi_i^\epsilon - \mathsf{G}_i\nabla_{\mathbf{y}}\phi_i^\epsilon \quad \text{in} \quad \Omega_i, \tag{31c}$$

$$\epsilon\mathbf{j}_e^\epsilon = -\epsilon\mathsf{G}_e\nabla_{\mathbf{x}}\phi_e^\epsilon - \mathsf{G}_e\nabla_{\mathbf{y}}\phi_e^\epsilon \quad \text{in} \quad \Omega_e, \tag{31d}$$

$$\epsilon\nabla_{\mathbf{x}}\cdot\mathsf{T}_i^\epsilon+\nabla_{\mathbf{y}}\cdot\mathsf{T}_i^\epsilon=-\epsilon\mathsf{G}_i\nabla_{\mathbf{x}}\phi_i^\epsilon\times\mathbf{B}^\epsilon-\mathsf{G}_i\nabla_{\mathbf{y}}\phi_i^\epsilon\times\mathbf{B}^\epsilon \quad \text{in} \quad \Omega_i, \tag{31e}$$

$$\epsilon\nabla_{\mathbf{x}}\cdot\mathsf{T}_e^\epsilon+\nabla_{\mathbf{y}}\cdot\mathsf{T}_e^\epsilon=-\epsilon\mathsf{G}_e\nabla_{\mathbf{x}}\phi_e^\epsilon\times\mathbf{B}^\epsilon-\mathsf{G}_e\nabla_{\mathbf{y}}\phi_e^\epsilon\times\mathbf{B}^\epsilon \quad \text{in} \quad \Omega_e, \tag{31f}$$

$$\epsilon\mathsf{T}_i^\epsilon=\epsilon\mathbb{C}_i\xi_{\mathbf{x}}(\mathbf{u}_i^\epsilon)+\mathbb{C}_i\xi_{\mathbf{y}}(\mathbf{u}_i^\epsilon) \quad \text{in} \quad \Omega_i, \tag{31g}$$

$$\epsilon\mathsf{T}_e^\epsilon=\epsilon\mathbb{C}_e\xi_{\mathbf{x}}(\mathbf{u}_e^\epsilon)+\mathbb{C}_e\xi_{\mathbf{y}}(\mathbf{u}_e^\epsilon)-\epsilon\hat{\boldsymbol{\alpha}}_e p_p^\epsilon \quad \text{in} \quad \Omega_e, \tag{31h}$$

$$\epsilon\mathbf{w}_e^\epsilon=-\epsilon\mathsf{K}_e\nabla_{\mathbf{x}}p_p^\epsilon+\mathsf{K}_e\nabla_{\mathbf{y}}p_p^\epsilon \quad \text{in} \quad \Omega_e, \tag{31i}$$

$$\epsilon\frac{\dot{p}_p^\epsilon}{\mathcal{M}_e}=-\hat{\boldsymbol{\alpha}}_e:\xi_y\dot{\mathbf{u}}_e^\epsilon-\epsilon\hat{\boldsymbol{\alpha}}_e:\xi_x\dot{\mathbf{u}}_e^\epsilon-\nabla_y\cdot\mathbf{w}_e^\epsilon-\epsilon\nabla_x\cdot\mathbf{w}_e^\epsilon \quad \text{in} \quad \Omega_e, \tag{31j}$$

$$\epsilon\nabla_{\mathbf{x}}\cdot\mathsf{T}_{\mathrm{f}}^\epsilon+\nabla_{\mathbf{y}}\cdot\mathsf{T}_{\mathrm{f}}^\epsilon=0 \quad \text{in} \quad \Omega_{\mathrm{f}}, \tag{31k}$$

$$\mathsf{T}_{\mathrm{f}}^\epsilon=-p_{\mathrm{f}}^\epsilon\mathbf{I}+\epsilon\xi_{\mathbf{y}}(\mathbf{v}_{\mathrm{f}}^\epsilon)+\epsilon^2\xi_{\mathbf{x}}(\mathbf{v}_{\mathrm{f}}^\epsilon) \quad \text{in} \quad \Omega_{\mathrm{f}}, \tag{31l}$$

$$\epsilon\nabla_{\mathbf{x}}\cdot\mathbf{v}_{\mathrm{f}}^\epsilon+\nabla_{\mathbf{y}}\cdot\mathbf{v}_{\mathrm{f}}^\epsilon=0 \quad \text{in} \quad \Omega_{\mathrm{f}}, \tag{31m}$$

$$\epsilon^3\nabla_x^2\mathbf{v}_{\mathrm{f}}^\epsilon+\epsilon^2\nabla_x\cdot(\nabla_y\mathbf{v}_{\mathrm{f}}^\epsilon)+\epsilon^2\nabla_y\cdot(\nabla_x\mathbf{v}_{\mathrm{f}}^\epsilon)+\epsilon\nabla_y^2\mathbf{v}_{\mathrm{f}}^\epsilon=\nabla_y p_{\mathrm{f}}^\epsilon+\epsilon\nabla_x p_{\mathrm{f}}^\epsilon \quad \text{in} \quad \Omega_{\mathrm{f}}, \tag{31n}$$

$$\mathsf{T}_i^\epsilon\cdot\mathbf{n}_\Gamma=\mathsf{T}_e^\epsilon\cdot\mathbf{n}_\Gamma \quad \text{on} \quad \Gamma, \tag{31o}$$

$$\mathbf{u}_i^\epsilon=\mathbf{u}_e^\epsilon \quad \text{on} \quad \Gamma, \tag{31p}$$

$$\mathsf{G}_i\nabla_{\mathbf{y}}\phi_i^\epsilon\cdot\mathbf{n}_\Gamma+\epsilon\mathsf{G}_i\nabla_{\mathbf{x}}\phi_i^\epsilon\cdot\mathbf{n}_\Gamma=\mathsf{G}_e\nabla_{\mathbf{y}}\phi_e^\epsilon\cdot\mathbf{n}_\Gamma+\epsilon\mathsf{G}_e\nabla_{\mathbf{x}}\phi_e^\epsilon\cdot\mathbf{n}_\Gamma \quad \text{on} \quad \Gamma, \tag{31q}$$

$$\phi_i^\epsilon-\phi_e^\epsilon=V^\epsilon \quad \text{on} \quad \Gamma, \tag{31r}$$

$$\mathbf{w}_e^\epsilon\cdot\mathbf{n}_\Gamma=0 \quad \text{on} \quad \Gamma, \tag{31s}$$

$$\mathbf{w}_e^\epsilon\cdot\mathbf{n}_\gamma=\mathbf{w}_{\mathrm{f}}^\epsilon\cdot\mathbf{n}_\gamma \quad \text{on} \quad \gamma, \tag{31t}$$

$$\mathsf{T}_{\mathrm{f}}^\epsilon\mathbf{n}_\gamma=\mathsf{T}_e^\epsilon\mathbf{n}_\gamma \quad \text{on} \quad \gamma, \tag{31u}$$

$$\epsilon\mathbf{n}_\gamma\cdot(\mathsf{T}_{\mathrm{f}}^\epsilon\mathbf{n}_\gamma)+\frac{1}{L_p}(\mathbf{v}_{\mathrm{f}}^\epsilon-\dot{\mathbf{u}}_e^\epsilon)\cdot\mathbf{n}_\gamma=-\epsilon p_p^\epsilon \quad \text{on} \quad \gamma, \tag{31v}$$

$$\tau_\beta\cdot(\mathsf{T}_{\mathrm{f}}^\epsilon\mathbf{n}_\gamma)=-\epsilon\frac{\alpha}{\sqrt{k}}(\mathbf{v}_{\mathrm{f}}^\epsilon-\dot{\mathbf{u}}_e^\epsilon)\cdot\tau_\beta \quad \text{on} \quad \gamma, \tag{31w}$$

$$\mathsf{G}_e\nabla_{\mathbf{y}}\phi_e^\epsilon\cdot\mathbf{n}_\gamma+\epsilon\mathsf{G}_e\nabla_{\mathbf{x}}\phi_e^\epsilon\cdot\mathbf{n}_\gamma=0 \quad \text{on} \quad \gamma. \tag{31x}$$

Now that we have our multiple scales expansion we proceed by substituting power series of the type (28) into the appropriate fields in ((31a)–(31x)). We then will equate the coefficients of ϵ^l for $l=0,1,\dots$ in order to derive the macroscale model for the perfused myocardium in terms of the relevant leading (zero-th) order fields. In the case that a term in the asymptotic expansion retains a dependence on the microscale, we apply the integral average. This average is defined as

$$\langle\varphi\rangle_k=\frac{1}{|\Omega|}\int_{\Omega_i}\varphi(\mathbf{x},\mathbf{y},t)d\mathbf{y} \quad k=i,e,\mathrm{f}. \tag{32}$$

The integral average is performed over one representative periodic cell due to the assumption of $\mathbf{y}$-periodicity and $|\Omega|$ is the volume of the domain and the integration is performed over the microscale. We have that $|\Omega|=|\Omega_i|+|\Omega_e|+|\Omega_{\mathrm{f}}|$. We note that (32) represents a cell average.

Equating coefficients of ϵ^0

$$\nabla_{\mathbf{y}}\cdot(\mathsf{G}_i\nabla_{\mathbf{y}}\phi_i^{(0)})=0 \quad \text{in} \quad \Omega_i, \tag{33a}$$

$$\nabla_{\mathbf{y}}\cdot(\mathsf{G}_e\nabla_{\mathbf{y}}\phi_e^{(0)})=0 \quad \text{in} \quad \Omega_e, \tag{33b}$$

$$\mathsf{G}_i\nabla_{\mathbf{y}}\phi_i^{(0)}=0 \quad \text{in} \quad \Omega_i, \tag{33c}$$

$$\mathsf{G}_e\nabla_{\mathbf{y}}\phi_e^{(0)}=0 \quad \text{in} \quad \Omega_e, \tag{33d}$$

$$\nabla_{\mathbf{y}}\cdot\mathsf{T}_i^{(0)}=-\mathsf{G}_i\nabla_{\mathbf{y}}\phi_i^{(0)}\times\mathbf{B}^{(0)} \quad \text{in} \quad \Omega_i, \tag{33e}$$

$$\nabla_{\mathbf{y}}\cdot\mathsf{T}_e^{(0)}=-\mathsf{G}_e\nabla_{\mathbf{y}}\phi_e^{(0)}\times\mathbf{B}^{(0)} \quad \text{in} \quad \Omega_e, \tag{33f}$$

$$\mathbb{C}_i\xi_{\mathbf{y}}(\mathbf{u}_i^{(0)})=0 \quad \text{in} \quad \Omega_i, \tag{33g}$$

$$\mathbb{C}_e\xi_{\mathbf{y}}(\mathbf{u}_e^{(0)})=0 \quad \text{in} \quad \Omega_e, \tag{33h}$$

$$\mathsf{K}_e\nabla_{\mathbf{y}}p_p^{(0)}=0 \quad \text{in} \quad \Omega_e, \tag{33i}$$

$$-\hat{\boldsymbol{\alpha}}_e:\xi_y\dot{\mathbf{u}}_e^{(0)}-\nabla_y\cdot\mathbf{w}_e^{(0)}=0 \quad \text{in} \quad \Omega_e, \tag{33j}$$

$$\nabla_{\mathbf{y}}\cdot\mathsf{T}_{\mathrm{f}}^{(0)}=0 \quad \text{in} \quad \Omega_{\mathrm{f}}, \tag{33k}$$

$$\mathsf{T}_{\mathrm{f}}^{(0)}=-p_{\mathrm{f}}^{(0)}\mathbf{I} \quad \text{in} \quad \Omega_{\mathrm{f}}, \tag{33l}$$

$$\nabla_{\mathbf{y}}\cdot\mathbf{v}_{\mathrm{f}}^{(0)}=0 \quad \text{in} \quad \Omega_{\mathrm{f}}, \tag{33m}$$

$$\nabla_y p_{\mathrm{f}}^{(0)}=0 \quad \text{in} \quad \Omega_{\mathrm{f}}, \tag{33n}$$

$$\mathsf{T}_i^{(0)}\cdot\mathbf{n}_\Gamma=\mathsf{T}_e^{(0)}\cdot\mathbf{n}_\Gamma \quad \text{on} \quad \Gamma, \tag{33o}$$

$$\mathbf{u}_i^{(0)}=\mathbf{u}_e^{(0)} \quad \text{on} \quad \Gamma, \tag{33p}$$

$$\mathsf{G}_i\nabla_{\mathbf{y}}\phi_i^{(0)}\cdot\mathbf{n}_\Gamma=\mathsf{G}_e\nabla_{\mathbf{y}}\phi_e^{(0)}\cdot\mathbf{n}_\Gamma \quad \text{on} \quad \Gamma, \tag{33q}$$

$$\phi_i^{(0)} - \phi_e^{(0)} = V^{(0)} \quad \text{on} \quad \Gamma, \tag{33r}$$

$$\mathbf{w}_e^{(0)} \cdot \mathbf{n}_\Gamma = 0 \quad \text{on} \quad \Gamma, \tag{33s}$$

$$\mathbf{w}_e^{(0)} \cdot \mathbf{n}_\gamma = \mathbf{w}_\mathrm{f}^{(0)} \cdot \mathbf{n}_\gamma \quad \text{on} \quad \gamma, \tag{33t}$$

$$\mathsf{T}_\mathrm{f}^{(0)}\mathbf{n}_\gamma = \mathsf{T}_e^{(0)}\mathbf{n}_\gamma \quad \text{on} \quad \gamma, \tag{33u}$$

$$(\mathbf{v}_\mathrm{f}^{(0)} - \dot{\mathbf{u}}_e^{(0)}) \cdot \mathbf{n}_\gamma = 0 \quad \text{on} \quad \gamma, \tag{33v}$$

$$\tau_\beta \cdot (\mathsf{T}_\mathrm{f}^{(0)}\mathbf{n}_\gamma) = 0 \quad \text{on} \quad \gamma, \tag{33w}$$

$$\mathsf{G}_e \nabla_\mathbf{y} \phi_e^{(0)} \cdot \mathbf{n}_\gamma = 0 \quad \text{on} \quad \gamma.. \tag{33x}$$

Using (33g) and (33h) we can see that the leading order elastic displacements $\mathbf{u}_i^{(0)}$ and $\mathbf{u}_e^{(0)}$ are rigid body motions. We therefore have by $\mathbf{y}$-periodicity, that they do not depend on the microscale variable $\mathbf{y}$. We therefore write

$$\mathbf{u}_i^{(0)} = \mathbf{u}_i^{(0)}(\mathbf{x}, t) \quad \text{and} \quad \mathbf{u}_e^{(0)} = \mathbf{u}_e^{(0)}(\mathbf{x}, t). \tag{34}$$

Due to the interface condition (33p) on Γ we can use that

$$\mathbf{u}^{(0)} = \mathbf{u}_i^{(0)} = \mathbf{u}_e^{(0)}, \tag{35}$$

throughout the remainder of this work.

We also see from (33k), (33i) and (33l) that the leading order fluid pressure $p_\mathrm{f}^{(0)}$ and the leading order interstitial pore pressure $p_p^{(0)}$ do not depend on the microscale variable. That is

$$p_\mathrm{f}^{(0)} = p_\mathrm{f}^{(0)}(\mathbf{x}, t) \quad \text{and} \quad p_p^{(0)} = p_p^{(0)}(\mathbf{x}, t). \tag{36}$$

Since we made the assumption (29) that the difference in electric potentials $V^{(0)}$ is a given and does not depend on the microscale variable $\mathbf{y}$ we can write down the ϵ^0 problem for the leading order electric potentials $\phi_i{}^{(0)}$ and $\phi_e{}^{(0)}$. To make use of the assumption (29) We define a new variable,

$$\bar{\phi}_e^{(0)} = \phi_e^{(0)} + V^{(0)}. \tag{37}$$

and this allows us to write the ϵ^0 problem in terms of $\phi_i{}^{(0)}$ and the new variable $\bar{\phi}_e^{(0)}$

$$\nabla_\mathbf{y} \cdot (\mathsf{G}_i \nabla_\mathbf{y} \phi_i^{(0)}) = 0, \quad \text{in} \quad \Omega_i \tag{38a}$$

$$\nabla_\mathbf{y} \cdot (\mathsf{G}_e \nabla_\mathbf{y} \bar{\phi}_e^{(0)}) = 0, \quad \text{in} \quad \Omega_e \tag{38b}$$

$$\phi_i^{(0)} = \bar{\phi}_e^{(0)}, \quad \text{on} \quad \Gamma \tag{38c}$$

$$\mathsf{G}_i \nabla_\mathbf{y} \phi_i^{(0)} \cdot \mathbf{n}_\Gamma = \mathsf{G}_e \nabla_\mathbf{y} \bar{\phi}_e^{(0)} \cdot \mathbf{n}_\Gamma \quad \text{on} \quad \Gamma \tag{38d}$$

The Eqs. (38a)–(38d) represent a boundary value problem that is of linear-elastic type. It has no source terms in (38a) and (38b) and is equipped with the jump condition (38d) between the current densities and with the continuity condition between the zero order electric potentials (38c). This type of problem has only solutions which are constant with respect to the macroscale variable $\mathbf{y}$, this has been proved in Bakhvalov and Panasenko (2012) and Cioranescu and Donato (1999). This allows us to deduce that $\phi_i{}^{(0)}$ and $\hat{\phi}_e^{(0)}$ do not depend on the microscale variable $\mathbf{y}$. It then follows using (29) that both $\phi_i{}^{(0)}$ and $\phi_e{}^{(0)}$ do not depend on that microscale. We therefore have

$$\phi_i{}^{(0)} = \phi_i{}^{(0)}(\mathbf{x}, t) \quad \text{and} \quad \phi_e{}^{(0)} = \phi_e{}^{(0)}(\mathbf{x}, t) \tag{39}$$

Due to this result the balance Eqs. (33e) and (33f) can be rewritten as

$$\nabla_\mathbf{y} \cdot \mathsf{T}_i^{(0)} = 0, \tag{40a}$$

$$\nabla_\mathbf{y} \cdot \mathsf{T}_e^{(0)} = 0. \tag{40b}$$

We now equate the coefficients of ϵ^1

$$\nabla_\mathbf{y} \cdot (\mathsf{G}_i \nabla_\mathbf{x} \phi_i^{(0)}) + \nabla_\mathbf{y} \cdot (\mathsf{G}_i \nabla_\mathbf{y} \phi_i^{(1)}) = 0 \quad \text{in} \quad \Omega_i, \tag{41a}$$

$$\nabla_\mathbf{y} \cdot (\mathsf{G}_e \nabla_\mathbf{x} \phi_e^{(0)}) + \nabla_\mathbf{y} \cdot (\mathsf{G}_e \nabla_\mathbf{y} \phi_e^{(1)}) = 0 \quad \text{in} \quad \Omega_e, \tag{41b}$$

$$\mathbf{j}_i^{(0)} = -\mathsf{G}_i \nabla_\mathbf{x} \phi_i^{(0)} - \mathsf{G}_i \nabla_\mathbf{y} \phi_i^{(1)} \quad \text{in} \quad \Omega_i, \tag{41c}$$

$$\mathbf{j}_e^{(0)} = -\mathsf{G}_e \nabla_\mathbf{x} \phi_e^{(0)} - \mathsf{G}_e \nabla_\mathbf{y} \phi_e^{(1)} \quad \text{in} \quad \Omega_e, \tag{41d}$$

$$\nabla_\mathbf{x} \cdot \mathsf{T}_i^{(0)} + \nabla_\mathbf{y} \cdot \mathsf{T}_i^{(1)} = -\mathsf{G}_i \nabla_\mathbf{x} \phi_i^{(0)} \times \mathbf{B}^{(0)} - \mathsf{G}_i \nabla_\mathbf{y} \phi_i^{(1)} \times \mathbf{B}^{(0)} \quad \text{in} \quad \Omega_i, \tag{41e}$$

$$\nabla_\mathbf{x} \cdot \mathsf{T}_e^{(0)} + \nabla_\mathbf{y} \cdot \mathsf{T}_e^{(1)} = -\mathsf{G}_e \nabla_\mathbf{x} \phi_e^{(0)} \times \mathbf{B}^{(0)} - \mathsf{G}_e \nabla_\mathbf{y} \phi_e^{(1)} \times \mathbf{B}^{(0)} \quad \text{in} \quad \Omega_e, \tag{41f}$$

$$\mathsf{T}_i^{(0)} = \mathbb{C}_i \xi_\mathbf{x} \mathbf{u}_i^{(0)} + \mathbb{C}_i \xi_\mathbf{y} \mathbf{u}_i^{(1)} \quad \text{in} \quad \Omega_i, \tag{41g}$$

$$\mathsf{T}_e^{(0)} = \mathbb{C}_e \xi_\mathbf{x} \mathbf{u}_e^{(0)} + \mathbb{C}_e \xi_\mathbf{y} \mathbf{u}_e^{(1)} - \hat{\boldsymbol{\alpha}}_e p_p^{(0)} \quad \text{in} \quad \Omega_e, \tag{41h}$$

$$\mathbf{w}_e^{(0)} = -\mathsf{K}_e \nabla_\mathbf{x} p_p^{(0)} + \mathsf{K}_e \nabla_\mathbf{y} p_p^{(1)} \quad \text{in} \quad \Omega_e, \tag{41i}$$

$$\frac{\dot{p}_p^{(0)}}{\mathcal{M}_e} = -\hat{\boldsymbol{\alpha}}_e : \xi_y \dot{\mathbf{u}}_e^{(1)} - \hat{\boldsymbol{\alpha}}_e : \xi_x \dot{\mathbf{u}}^{(0)} - \nabla_y \cdot \mathbf{w}_e^{(1)} - \nabla_x \cdot \mathbf{w}_e^{(0)} \quad \text{in} \quad \Omega_e, \tag{41j}$$

$$\nabla_{\mathbf{x}} \cdot \mathsf{T}_{\mathrm{f}}^{(0)} + \nabla_{\mathbf{y}} \cdot \mathsf{T}_{\mathrm{f}}^{(1)} = 0 \quad \text{in} \quad \Omega_f, \tag{41k}$$

$$\mathsf{T}_{\mathrm{f}}^{(1)} = -p_{\mathrm{f}}^{(1)} \mathrm{I} + \xi_{\mathbf{y}}(\mathbf{v}_{\mathrm{f}}^{(0)}) \quad \text{in} \quad \Omega_f, \tag{41l}$$

$$\nabla_{\mathbf{x}} \cdot \mathbf{v}_{\mathrm{f}}^{(0)} + \nabla_{\mathbf{y}} \cdot \mathbf{v}_{\mathrm{f}}^{(1)} = 0 \quad \text{in} \quad \Omega_f, \tag{41m}$$

$$\nabla_y^2 \mathbf{v}_{\mathrm{f}}^{(0)} = \nabla_y p_{\mathrm{f}}^{(1)} + \nabla_x p_{\mathrm{f}}^{(0)} \quad \text{in} \quad \Omega_f, \tag{41n}$$

$$\mathsf{T}_i^{(1)} \cdot \mathbf{n}_\Gamma = \mathsf{T}_e^{(1)} \cdot \mathbf{n}_\Gamma \quad \text{on} \quad \Gamma, \tag{41o}$$

$$\mathbf{u}_i^{(1)} = \mathbf{u}_e^{(1)} \quad \text{on} \quad \Gamma, \tag{41p}$$

$$\mathsf{G}_i \nabla_{\mathbf{y}} \phi_i^{(1)} \cdot \mathbf{n}_\Gamma + \mathsf{G}_i \nabla_{\mathbf{x}} \phi_i^{(0)} \cdot \mathbf{n}_\Gamma = \mathsf{G}_e \nabla_{\mathbf{y}} \phi_e^{(1)} \cdot \mathbf{n}_\Gamma + \mathsf{G}_e \nabla_{\mathbf{x}} \phi_e^{(0)} \cdot \mathbf{n}_\Gamma \quad \text{on} \quad \Gamma, \tag{41q}$$

$$\phi_i^{(1)} - \phi_e^{(1)} = V^{(1)} \quad \text{on} \quad \Gamma, \tag{41r}$$

$$\mathbf{w}_e^{(1)} \cdot \mathbf{n}_\Gamma = 0 \quad \text{on} \quad \Gamma, \tag{41s}$$

$$\mathbf{w}_e^{(1)} \cdot \mathbf{n}_\gamma = \mathbf{w}_{\mathrm{f}}^{(1)} \cdot \mathbf{n}_\gamma \quad \text{on} \quad \gamma, \tag{41t}$$

$$\mathsf{T}_{\mathrm{f}}^{(1)} \mathbf{n}_\gamma = \mathsf{T}_e^{(1)} \mathbf{n}_\gamma \quad \text{on} \quad \gamma, \tag{41u}$$

$$\mathbf{n}_\gamma \cdot (\mathsf{T}_{\mathrm{f}}^{(0)} \mathbf{n}_\gamma) + \frac{1}{L_p} (\mathbf{v}_{\mathrm{f}}^{(1)} - \dot{\mathbf{u}}_e^{(1)}) \cdot \mathbf{n}_\gamma = -p_p^{(0)} \quad \text{on} \quad \gamma, \tag{41v}$$

$$\tau_\beta \cdot (\mathsf{T}_{\mathrm{f}}^{(1)} \mathbf{n}_\gamma) = -\frac{\alpha}{\sqrt{k}} (\mathbf{v}_{\mathrm{f}}^{(0)} - \dot{\mathbf{u}}_e^{(0)}) \cdot \tau_\beta \quad \text{on} \quad \gamma, \tag{41w}$$

$$\mathsf{G}_e \nabla_{\mathbf{y}} \phi_e^{(1)} \cdot \mathbf{n}_\gamma + \mathsf{G}_e \nabla_{\mathbf{x}} \phi_e^{(0)} \cdot \mathbf{n}_\gamma = 0 \quad \text{on} \quad \gamma. \tag{41x}$$

With the equated coefficients of powers 0 and 1 of ϵ we will now form problems for the order 1 electric potentials, elastic displacements and the relative fluid–solid velocities.

3.4. Problem for electric potentials $\phi_i^{(1)}$ and $\phi_e^{(1)}$

By taking the Eqs. (41a), (41b), (41r), (41q) and (41x) we can write the following problem for the electric potentials $\phi_i^{(1)}$ and $\phi_e^{(1)}$. We have,

$$\nabla_{\mathbf{y}} \cdot (\mathsf{G}_i \nabla_{\mathbf{x}} \phi_i^{(0)}) + \nabla_{\mathbf{y}} \cdot (\mathsf{G}_i \nabla_{\mathbf{y}} \phi_i^{(1)}) = 0 \quad \text{in} \quad \Omega_i, \tag{42a}$$

$$\nabla_{\mathbf{y}} \cdot (\mathsf{G}_e \nabla_{\mathbf{x}} \phi_e^{(0)}) + \nabla_{\mathbf{y}} \cdot (\mathsf{G}_e \nabla_{\mathbf{y}} \phi_e^{(1)}) = 0 \quad \text{in} \quad \Omega_e, \tag{42b}$$

$$\phi_i^{(1)} - \phi_e^{(1)} = V^{(1)} \quad \text{on} \quad \Gamma, \tag{42c}$$

$$(\mathsf{G}_i \nabla_{\mathbf{y}} \phi_i^{(1)} - \mathsf{G}_e \nabla_{\mathbf{y}} \phi_e^{(1)}) \cdot \mathbf{n}_\Gamma = (\mathsf{G}_e \nabla_{\mathbf{x}} \phi_e^{(0)} - \mathsf{G}_i \nabla_{\mathbf{x}} \phi_i^{(0)}) \cdot \mathbf{n}_\Gamma \quad \text{on} \quad \Gamma. \tag{42d}$$

$$(\mathsf{G}_e \nabla_{\mathbf{y}} \phi_e^{(1)} - \mathsf{G}_e \nabla_{\mathbf{x}} \phi_e^{(0)}) \cdot \mathbf{n}_\gamma = 0 \quad \text{on} \quad \gamma \tag{42e}$$

We exploit the linearity of problem (42a)–(42e) to propose the ansatz

$$\phi_i^{(1)} = \boldsymbol{\Phi}_i \cdot \nabla_{\mathbf{x}} \phi_i^{(0)} + \hat{\boldsymbol{\Phi}}_i \cdot \nabla_{\mathbf{x}} \phi_e^{(0)} + \tilde{\phi}_i, \tag{43a}$$

$$\phi_e^{(1)} = \boldsymbol{\Phi}_e \cdot \nabla_{\mathbf{x}} \phi_e^{(0)} + \hat{\boldsymbol{\Phi}}_e \cdot \nabla_{\mathbf{x}} \phi_i^{(0)} + \tilde{\phi}_e, \tag{43b}$$

where we have that $\boldsymbol{\Phi}_i$, $\boldsymbol{\Phi}_e$, $\hat{\boldsymbol{\Phi}}_i$ and $\hat{\boldsymbol{\Phi}}_e$ are vectors and $\tilde{\phi}_i$ and $\tilde{\phi}_e$ are scalars. We have that these auxiliary fields $\boldsymbol{\Phi}_i$, $\boldsymbol{\Phi}_e$, $\hat{\boldsymbol{\Phi}}_i$, $\hat{\boldsymbol{\Phi}}_e$, $\tilde{\phi}_i$ and $\tilde{\phi}_e$ satisfy the following cell problems

$$\nabla_{\mathbf{y}} \cdot (\nabla_{\mathbf{y}} \boldsymbol{\Phi}_i \mathsf{G}_i^{\mathrm{T}}) + \nabla_{\mathbf{y}} \cdot \mathsf{G}_i^{\mathrm{T}} = \mathbf{0} \quad \text{in} \quad \Omega_i, \tag{44a}$$

$$\nabla_{\mathbf{y}} \cdot (\nabla_{\mathbf{y}} \hat{\boldsymbol{\Phi}}_e \mathsf{G}_e^{\mathrm{T}}) = \mathbf{0} \quad \text{in} \quad \Omega_e, \tag{44b}$$

$$\boldsymbol{\Phi}_i = \hat{\boldsymbol{\Phi}}_e \quad \text{on} \quad \Gamma, \tag{44c}$$

$$(\nabla_{\mathbf{y}} \boldsymbol{\Phi}_i \mathsf{G}_i^{\mathrm{T}} - \nabla_{\mathbf{y}} \hat{\boldsymbol{\Phi}}_e \mathsf{G}_e^{\mathrm{T}}) \cdot \mathbf{n}_\Gamma = -\mathsf{G}_i^{\mathrm{T}} \cdot \mathbf{n}_\Gamma \quad \text{on} \quad \Gamma, \tag{44d}$$

$$(\nabla_{\mathbf{y}} \hat{\boldsymbol{\Phi}}_e \mathsf{G}_e^{\mathrm{T}}) \cdot \mathbf{n}_\gamma = \mathbf{0} \quad \text{on} \quad \gamma \tag{44e}$$

and

$$\nabla_{\mathbf{y}} \cdot (\nabla_{\mathbf{y}} \hat{\boldsymbol{\Phi}}_i \mathsf{G}_i^{\mathrm{T}}) = \mathbf{0} \quad \text{in} \quad \Omega_i, \tag{45a}$$

$$\nabla_{\mathbf{y}} \cdot (\nabla_{\mathbf{y}} \boldsymbol{\Phi}_e \mathsf{G}_e^{\mathrm{T}}) + \nabla_{\mathbf{y}} \cdot \mathsf{G}_e^{\mathrm{T}} = \mathbf{0} \quad \text{in} \quad \Omega_e, \tag{45b}$$

$$\hat{\boldsymbol{\Phi}}_i = \boldsymbol{\Phi}_e \quad \text{on} \quad \Gamma, \tag{45c}$$

$$(\nabla_{\mathbf{y}} \hat{\boldsymbol{\Phi}}_i \mathsf{G}_i^{\mathrm{T}} - \nabla_{\mathbf{y}} \boldsymbol{\Phi}_e \mathsf{G}_e^{\mathrm{T}}) \cdot \mathbf{n}_\Gamma = \mathsf{G}_e^{\mathrm{T}} \cdot \mathbf{n}_\Gamma \quad \text{on} \quad \Gamma, \tag{45d}$$

$$\nabla_{\mathbf{y}} \boldsymbol{\Phi}_e \mathsf{G}_e^{\mathrm{T}} \cdot \mathbf{n}_\gamma = \mathsf{G}_e^{\mathrm{T}} \cdot \mathbf{n}_\gamma \quad \text{on} \quad \gamma \tag{45e}$$

and

$$\nabla_{\mathbf{y}} \cdot (\mathsf{G}_i \nabla_{\mathbf{y}} \tilde{\phi}_i) = 0 \quad \text{in} \quad \Omega_i, \tag{46a}$$

$$\nabla_{\mathbf{y}} \cdot (\mathsf{G}_e \nabla_{\mathbf{y}} \tilde{\phi}_e) = 0 \quad \text{in} \quad \Omega_e, \tag{46b}$$

$$\tilde{\phi}_i - \tilde{\phi}_e = V^{(1)} \quad \text{on} \quad \Gamma, \tag{46c}$$

$$(\mathsf{G}_i\nabla_{\mathbf{y}}\tilde{\phi}_i)\cdot\mathbf{n}_\Gamma = (\mathsf{G}_e\nabla_{\mathbf{y}}\tilde{\phi}_e)\cdot\mathbf{n}_\Gamma \qquad \text{on} \quad \Gamma. \tag{46d}$$

$$(\mathsf{G}_e\nabla_{\mathbf{y}}\tilde{\phi}_e)\cdot\mathbf{n}_\gamma = 0 \qquad \text{on} \quad \gamma \tag{46e}$$

where there are periodic conditions on the boundary $\partial\Omega\setminus\Gamma\cup\gamma$ and to ensure uniqueness of solution we require a further condition on the auxiliary fields $\boldsymbol{\Phi}_i$, $\boldsymbol{\Phi}_e$, $\hat{\boldsymbol{\Phi}}_i$, $\hat{\boldsymbol{\Phi}}_e$, $\tilde{\phi}_i$ and $\tilde{\phi}_e$. We propose zero average in their respective domains, that is

$$\langle\boldsymbol{\Phi}_i\rangle_i = 0, \quad \langle\boldsymbol{\Phi}_e\rangle_e = 0, \quad \langle\hat{\boldsymbol{\Phi}}_i\rangle_i = 0, \quad \langle\hat{\boldsymbol{\Phi}}_e\rangle_e = 0, \quad \langle\tilde{\phi}_i\rangle_i = 0, \quad \langle\tilde{\phi}_e\rangle_e = 0. \tag{47}$$

As we have expressions for $\phi_i^{(1)}$ and $\phi_e^{(1)}$ from (43a) and (43b) we can write down the leading order Ohm's law for the current densities $\mathbf{j}_i^{(0)}$ and $\mathbf{j}_e^{(0)}$ (Eqs. (41c) and (41d)) as

$$\begin{aligned}\mathbf{j}_i^{(0)} &= -\mathsf{G}_i\nabla_{\mathbf{x}}\phi_i^{(0)} - \mathsf{G}_i\nabla_{\mathbf{y}}\phi_i^{(1)}\\ &= -(\mathsf{G}_i + \mathsf{G}_i(\nabla_{\mathbf{y}}\boldsymbol{\Phi}_i)^{\mathrm{T}})\nabla_{\mathbf{x}}\phi_i^{(0)} - \mathsf{G}_i(\nabla_{\mathbf{y}}\hat{\boldsymbol{\Phi}}_i)^{\mathrm{T}}\nabla_{\mathbf{x}}\phi_e^{(0)} - \mathsf{G}_i\nabla_{\mathbf{y}}\tilde{\phi}_i\\ &= -(\mathsf{G}_i + \mathsf{G}_i\mathsf{R}_i)\nabla_{\mathbf{x}}\phi_i^{(0)} - (\mathsf{G}_i\mathsf{Q}_i)\nabla_{\mathbf{x}}\phi_e^{(0)} - \mathsf{G}_i\mathbf{s}_i\end{aligned} \tag{48}$$

and

$$\begin{aligned}\mathbf{j}_e^{(0)} &= -\mathsf{G}_e\nabla_{\mathbf{x}}\phi_e^{(0)} - \mathsf{G}_e\nabla_{\mathbf{y}}\phi_e^{(1)}\\ &= -(\mathsf{G}_e + \mathsf{G}_e(\nabla_{\mathbf{y}}\boldsymbol{\Phi}_e)^{\mathrm{T}})\nabla_{\mathbf{x}}\phi_e^{(0)} - \mathsf{G}_e(\nabla_{\mathbf{y}}\hat{\boldsymbol{\Phi}}_e)^{\mathrm{T}}\nabla_{\mathbf{x}}\phi_i^{(0)} - \mathsf{G}_e\nabla_{\mathbf{y}}\tilde{\phi}_e\\ &= -(\mathsf{G}_e + \mathsf{G}_e\mathsf{R}_e)\nabla_{\mathbf{x}}\phi_e^{(0)} - (\mathsf{G}_e\mathsf{Q}_e)\nabla_{\mathbf{x}}\phi_i^{(0)} - \mathsf{G}_e\mathbf{s}_e\end{aligned} \tag{49}$$

where for convenience and readability we have used the notation

$$\mathsf{R}_i = (\nabla_{\mathbf{y}}\boldsymbol{\Phi}_i)^{\mathrm{T}}, \quad \mathsf{R}_e = (\nabla_{\mathbf{y}}\boldsymbol{\Phi}_e)^{\mathrm{T}}, \quad \mathsf{Q}_i = (\nabla_{\mathbf{y}}\hat{\boldsymbol{\Phi}}_i)^{\mathrm{T}}, \quad \mathsf{Q}_e = (\nabla_{\mathbf{y}}\hat{\boldsymbol{\Phi}}_e)^{\mathrm{T}}, \quad \mathbf{s}_i = \nabla_{\mathbf{y}}\tilde{\phi}_i, \quad \mathbf{s}_e = \nabla_{\mathbf{y}}\tilde{\phi}_e. \tag{50}$$

To govern the current densities on the macroscale we require a balance equation. To do this we need to equate the coefficients of ϵ^2 in (31a) and (31b) and use the ϵ^2 definition of (31c) and (31d). We have

$$\nabla_{\mathbf{x}}\cdot(\mathsf{G}_i\nabla_{\mathbf{x}}\phi_i^{(0)}) + \nabla_{\mathbf{x}}\cdot(\mathsf{G}_i\nabla_{\mathbf{y}}\phi_i^{(1)}) + \nabla_{\mathbf{y}}\cdot(\mathsf{G}_i\nabla_{\mathbf{x}}\phi_i^{(1)}) + \nabla_{\mathbf{y}}\cdot(\mathsf{G}_i\nabla_{\mathbf{y}}\phi_i^{(2)}) = \hat{\beta}(\phi_i^{(0)} - \phi_e^{(0)}) - I_i^{(0)}, \tag{51a}$$

$$\nabla_{\mathbf{x}}\cdot(\mathsf{G}_e\nabla_{\mathbf{x}}\phi_e^{(0)}) + \nabla_{\mathbf{x}}\cdot(\mathsf{G}_e\nabla_{\mathbf{y}}\phi_e^{(1)}) + \nabla_{\mathbf{y}}\cdot(\mathsf{G}_e\nabla_{\mathbf{x}}\phi_e^{(1)}) + \nabla_{\mathbf{y}}\cdot(\mathsf{G}_e\nabla_{\mathbf{y}}\phi_e^{(2)}) = -\hat{\beta}(\phi_i^{(0)} - \phi_e^{(0)}) - I_e^{(0)}, \tag{51b}$$

with the coefficient of the ϵ^2 terms in the expansions of Ohm's law

$$\mathbf{j}_i^{(1)} = -\mathsf{G}_i\nabla_{\mathbf{x}}\phi_i^{(1)} - \mathsf{G}_i\nabla_{\mathbf{y}}\phi_i^{(2)}, \tag{52a}$$

$$\mathbf{j}_e^{(1)} = -\mathsf{G}_e\nabla_{\mathbf{x}}\phi_e^{(1)} - \mathsf{G}_e\nabla_{\mathbf{y}}\phi_e^{(2)}. \tag{52b}$$

We can then use the expressions for the order 1 current densities (52a) and (52b), along with the leading order current densities (41c) and (41d) in (51a) and (51b) to obtain

$$\nabla_{\mathbf{x}}\cdot\mathbf{j}_i^{(0)} + \nabla_{\mathbf{y}}\cdot\mathbf{j}_i^{(1)} = \hat{\beta}(\phi_i^{(0)} - \phi_e^{(0)}) - I_i^{(0)}, \tag{53a}$$

$$\nabla_{\mathbf{x}}\cdot\mathbf{j}_e^{(0)} + \nabla_{\mathbf{y}}\cdot\mathbf{j}_e^{(1)} = -\hat{\beta}(\phi_i^{(0)} - \phi_e^{(0)}) - I_e^{(0)}. \tag{53b}$$

We also consider the ϵ^2 expansions of interface conditions (31q) and (31x)

$$(\mathsf{G}_i\nabla_{\mathbf{x}}\phi_i^{(1)} + \mathsf{G}_i\nabla_{\mathbf{y}}\phi_i^{(2)})\cdot\mathbf{n}_\Gamma = (\mathsf{G}_e\nabla_{\mathbf{x}}\phi_e^{(1)} + \mathsf{G}_e\nabla_{\mathbf{y}}\phi_e^{(2)})\cdot\mathbf{n}_\Gamma, \tag{54a}$$

$$(\mathsf{G}_e\nabla_{\mathbf{x}}\phi_e^{(1)} + \mathsf{G}_e\nabla_{\mathbf{y}}\phi_e^{(2)})\cdot\mathbf{n}_\gamma = 0, \tag{54b}$$

which when using (52a) and (52b) can be written as

$$\mathbf{j}_i^{(1)}\cdot\mathbf{n}_\Gamma = \mathbf{j}_e^{(1)}\cdot\mathbf{n}_\Gamma, \tag{55a}$$

$$\mathbf{j}_e^{(1)}\cdot\mathbf{n}_\gamma = 0. \tag{55b}$$

We can take the integral average of the sum of (53a) and (53b) which gives

$$\int_{\Omega_i}\nabla_{\mathbf{x}}\cdot\mathbf{j}_i^{(0)}\mathrm{d}\mathbf{y} + \int_{\Omega_i}\nabla_{\mathbf{y}}\cdot\mathbf{j}_i^{(1)}\mathrm{d}\mathbf{y} - \int_{\Omega_i}\hat{\beta}(\phi_i^{(0)} - \phi_e^{(0)})\mathrm{d}\mathbf{y} + \int_{\Omega_e}\nabla_{\mathbf{x}}\cdot\mathbf{j}_e^{(0)}\mathrm{d}\mathbf{y} + \int_{\Omega_e}\nabla_{\mathbf{y}}\cdot\mathbf{j}_e^{(1)}\mathrm{d}\mathbf{y} + \int_{\Omega_e}\hat{\beta}(\phi_i^{(0)} - \phi_e^{(0)})\mathrm{d}\mathbf{y} + \int_{\Omega_i}I_i^{(0)}\mathrm{d}\mathbf{y} + \int_{\Omega_e}I_e^{(0)}\mathrm{d}\mathbf{y} = 0 \tag{56}$$

We apply macroscopic uniformity to the first and third integrals and the divergence theorem to the second and fourth integrals and we obtain

$$\begin{aligned}&\nabla_{\mathbf{x}}\cdot\langle\mathbf{j}_i^{(0)}\rangle_i + \nabla_{\mathbf{x}}\cdot\langle\mathbf{j}_e^{(0)}\rangle_e + \int_{\partial\Omega_i\setminus\Gamma}\mathbf{j}_i^{(1)}\mathbf{n}_{\partial\Omega_i}\mathrm{d}S + \int_\Gamma\mathbf{j}_i^{(1)}\mathbf{n}_\Gamma\mathrm{d}S + \int_{\partial\Omega_e\setminus\Gamma\cup\gamma}\mathbf{j}_e^{(1)}\mathbf{n}_{\partial\Omega_e}\mathrm{d}S - \int_\Gamma\mathbf{j}_e^{(1)}\mathbf{n}_\Gamma\mathrm{d}S - \int_\gamma\mathbf{j}_e^{(1)}\mathbf{n}_\gamma\mathrm{d}S - \int_{\Omega_i}\hat{\beta}(\phi_i^{(0)} - \phi_e^{(0)})\mathrm{d}\mathbf{y} + \int_{\Omega_e}\hat{\beta}(\phi_i^{(0)} - \phi_e^{(0)})\mathrm{d}\mathbf{y}\\ &+ \int_{\Omega_i}I_i^{(0)}\mathrm{d}\mathbf{y} + \int_{\Omega_e}I_e^{(0)}\mathrm{d}\mathbf{y} = 0.\end{aligned} \tag{57}$$

The terms on the external boundaries will cancel out due to periodicity and using the interface conditions (55a) and (55b) we see that the terms on Γ and γ will also disappear. This leaves

$$\nabla_{\mathbf{x}}\cdot\langle\mathbf{j}_i^{(0)}\rangle_i + \nabla_{\mathbf{x}}\cdot\langle\mathbf{j}_e^{(0)}\rangle_e - \int_{\Omega_i}\hat{\beta}(\phi_i^{(0)} - \phi_e^{(0)})\mathrm{d}\mathbf{y} + \int_{\Omega_e}\hat{\beta}(\phi_i^{(0)} - \phi_e^{(0)})\mathrm{d}\mathbf{y} + \int_{\Omega_i}I_i^{(0)}\mathrm{d}\mathbf{y} + \int_{\Omega_e}I_e^{(0)}\mathrm{d}\mathbf{y} = 0. \tag{58}$$

Since we have (33r) and the leading order electric potentials (39) do not depend on the microscale we can rewrite (58) as

$$\nabla_{\mathbf{x}}\cdot\langle\mathbf{j}_i^{(0)}\rangle_i + \nabla_{\mathbf{x}}\cdot\langle\mathbf{j}_e^{(0)}\rangle_e - \hat{\beta}V^{(0)}(|\Omega_e| - |\Omega_i|) + |\Omega_e|I_i + |\Omega_i|I_e = 0. \tag{59}$$

where we have that

$$\langle \mathbf{j}_i^{(0)} \rangle_i = -\langle \mathsf{G}_i + \mathsf{G}_i\mathsf{R}_i \rangle_i \nabla_{\mathbf{x}} \phi_i^{(0)} - \langle \mathsf{G}_i\mathsf{Q}_i \rangle_i \nabla_{\mathbf{x}} \phi_e^{(0)} - \langle \mathsf{G}_i \mathbf{s}_i \rangle_i \tag{60a}$$

$$\langle \mathbf{j}_e^{(0)} \rangle_e = -\langle \mathsf{G}_e + \mathsf{G}_e\mathsf{R}_e \rangle_e \nabla_{\mathbf{x}} \phi_e^{(0)} - \langle \mathsf{G}_e\mathsf{Q}_e \rangle_e \nabla_{\mathbf{x}} \phi_i^{(0)} - \langle \mathsf{G}_e \mathbf{s}_e \rangle_e \tag{60b}$$

3.5. Problem for the poromechanics

We now investigate the elastic displacements $\mathbf{u}_i^{(1)}$ and $\mathbf{u}_e^{(1)}$. By using balance Eqs. (40a), (40b) with leading order stresses (41g) and (41h) along with the interface conditions (41p), (33o) and (33u) using (33l) we can write

$$\nabla_{\mathbf{y}} \cdot (\mathbb{C}_i \xi_{\mathbf{x}}(\mathbf{u}^{(0)})) + \nabla_{\mathbf{y}} \cdot (\mathbb{C}_i \xi_{\mathbf{y}}(\mathbf{u}_i^{(1)})) = 0 \quad \text{in} \quad \Omega_i, \tag{61a}$$

$$\nabla_{\mathbf{y}} \cdot (\mathbb{C}_e \xi_{\mathbf{x}}(\mathbf{u}^{(0)})) + \nabla_{\mathbf{y}} \cdot (\mathbb{C}_e \xi_{\mathbf{y}}(\mathbf{u}_e^{(1)})) = -\nabla_{\mathbf{y}} \cdot (p_p^{(0)} \hat{\boldsymbol{\alpha}}_e) \quad \text{in} \quad \Omega_e, \tag{61b}$$

$$\mathbf{u}_i^{(1)} = \mathbf{u}_e^{(1)} \quad \text{on} \quad \Gamma, \tag{61c}$$

$$(\mathbb{C}_i \xi_{\mathbf{y}}(\mathbf{u}_i^{(1)}) - \mathbb{C}_e \xi_{\mathbf{y}}(\mathbf{u}_e^{(1)}) - \hat{\boldsymbol{\alpha}}_e p_p^{(0)}) \mathbf{n}_\Gamma = (\mathbb{C}_e - \mathbb{C}_i) \xi_{\mathbf{x}}(\mathbf{u}^{(0)}) \mathbf{n}_\Gamma \quad \text{on} \quad \Gamma, \tag{61d}$$

$$(\mathbb{C}_e \xi_y(\mathbf{u}_e^{(1)}) + \mathbb{C}_e \xi_x(\mathbf{u}^{(0)}) - \hat{\boldsymbol{\alpha}}_e p_p^{(0)}) \mathbf{n}_\gamma = -p_{\mathrm{f}}^{(0)} \mathbf{n}_\gamma \quad \text{on} \quad \gamma. \tag{61e}$$

We exploit the linearity of the problem and propose the ansatz

$$\mathbf{u}_i^{(1)} = \mathcal{A}_i \xi_{\mathbf{x}} \mathbf{u}^{(0)} + \mathbf{a}_i p_p^{(0)} + \mathbf{b}_i p_{\mathrm{f}}^{(0)}, \tag{62a}$$

$$\mathbf{u}_e^{(1)} = \mathcal{A}_e \xi_{\mathbf{x}} \mathbf{u}^{(0)} + \mathbf{a}_e p_p^{(0)} + \mathbf{b}_e p_{\mathrm{f}}^{(0)}, \tag{62b}$$

where $\mathcal{A}_i$ and $\mathcal{A}_e$ are third rank tensors and $\mathbf{a}_i$, $\mathbf{a}_e$, $\mathbf{b}_i$ and $\mathbf{b}_e$ are vectors which solve the following cell problems

$$\nabla_{\mathbf{y}} \cdot (\mathbb{C}_i \xi_{\mathbf{y}}(\mathcal{A}_i)) + \nabla_{\mathbf{y}} \cdot \mathbb{C}_i = 0 \quad \text{in} \quad \Omega_i, \tag{63a}$$

$$\nabla_{\mathbf{y}} \cdot (\mathbb{C}_e \xi_{\mathbf{y}}(\mathcal{A}_e)) + \nabla_{\mathbf{y}} \cdot \mathbb{C}_e = 0 \quad \text{in} \quad \Omega_e, \tag{63b}$$

$$\mathcal{A}_i = \mathcal{A}_e \quad \text{on} \quad \Gamma, \tag{63c}$$

$$(\mathbb{C}_i \xi_{\mathbf{y}}(\mathcal{A}_i) - \mathbb{C}_e \xi_{\mathbf{y}}(\mathcal{A}_e)) \mathbf{n}_\Gamma = (\mathbb{C}_e - \mathbb{C}_i) \mathbf{n}_\Gamma \quad \text{on} \quad \Gamma, \tag{63d}$$

$$(\mathbb{C}_e \xi_y(\mathcal{A}_e)) \mathbf{n}_\gamma = -\mathbb{C}_e \mathbf{n}_\gamma \quad \text{on} \quad \gamma. \tag{63e}$$

and

$$\nabla_{\mathbf{y}} \cdot (\mathbb{C}_i \xi_{\mathbf{y}} \mathbf{a}_i) = \mathbf{0} \quad \text{in} \quad \Omega_i, \tag{64a}$$

$$\nabla_{\mathbf{y}} \cdot (\mathbb{C}_e \xi_{\mathbf{y}} \mathbf{a}_e) = -\nabla_{\mathbf{y}} \cdot \hat{\boldsymbol{\alpha}}_e \quad \text{in} \quad \Omega_e, \tag{64b}$$

$$\mathbf{a}_i = \mathbf{a}_e \quad \text{on} \quad \Gamma, \tag{64c}$$

$$(\mathbb{C}_i \xi_{\mathbf{y}} \mathbf{a}_i - \mathbb{C}_e \xi_{\mathbf{y}} \mathbf{a}_e - \hat{\boldsymbol{\alpha}}_e) \mathbf{n}_\Gamma = \mathbf{0} \quad \text{on} \quad \Gamma, \tag{64d}$$

$$(\mathbb{C}_e \xi_y(\mathbf{a}_e) - \hat{\boldsymbol{\alpha}}_e) \mathbf{n}_\gamma + \mathbf{n}_\gamma = \mathbf{0} \quad \text{on} \quad \gamma. \tag{64e}$$

and

$$\nabla_{\mathbf{y}} \cdot (\mathbb{C}_i \xi_{\mathbf{y}} \mathbf{b}_i) = \mathbf{0} \quad \text{in} \quad \Omega_i, \tag{65a}$$

$$\nabla_{\mathbf{y}} \cdot (\mathbb{C}_e \xi_{\mathbf{y}} \mathbf{b}_e) = \mathbf{0} \quad \text{in} \quad \Omega_e, \tag{65b}$$

$$\mathbf{b}_i = \mathbf{b}_e \quad \text{on} \quad \Gamma, \tag{65c}$$

$$(\mathbb{C}_i \xi_{\mathbf{y}} \mathbf{b}_i - \mathbb{C}_e \xi_{\mathbf{y}} \mathbf{b}_e) \mathbf{n}_\Gamma = \mathbf{0} \quad \text{on} \quad \Gamma, \tag{65d}$$

$$(\mathbb{C}_e \xi_y(\mathbf{b}_e)) \mathbf{n}_\gamma = -\mathbf{n}_\gamma \quad \text{on} \quad \gamma. \tag{65e}$$

For uniqueness of solution we require an additional condition on the auxiliary tensors $\mathcal{A}_i$ and $\mathcal{A}_e$ and the vectors $\mathbf{a}_i$, $\mathbf{a}_e$, $\mathbf{b}_i$ and $\mathbf{b}_e$ so we propose

$$\langle \mathcal{A}_i \rangle_i = 0, \quad \langle \mathcal{A}_e \rangle_e = 0, \quad \langle \mathbf{a}_i \rangle_i = 0, \quad \langle \mathbf{a}_e \rangle_e = 0, \quad \langle \mathbf{b}_i \rangle_i = 0 \quad \text{and} \quad \langle \mathbf{b}_e \rangle_e = 0. \tag{66}$$

Now that we have the expressions for the order 1 elastic displacements $\mathbf{u}_i^{(1)}$ and $\mathbf{u}_e^{(1)}$ we can write the leading order stresses (41g) and (41h) as

$$\begin{aligned} \mathsf{T}_i^{(0)} &= \mathbb{C}_i \xi_{\mathbf{x}} \mathbf{u}^{(0)} + \mathbb{C}_i \xi_{\mathbf{y}} \mathcal{A}_i \xi_{\mathbf{x}} \mathbf{u}^{(0)} + \mathbb{C}_i \xi_{\mathbf{y}} \mathbf{a}_i p_p^{(0)} + \mathbb{C}_i \xi_{\mathbf{y}} \mathbf{b}_i p_{\mathrm{f}}^{(0)} \\ &= (\mathbb{C}_i + \mathbb{C}_i \mathbb{M}_i) \xi_{\mathbf{x}} \mathbf{u}^{(0)} + \mathbb{C}_i \mathsf{L}_i p_p^{(0)} + \mathbb{C}_i \mathsf{N}_i p_{\mathrm{f}}^{(0)}, \end{aligned} \tag{67}$$

and

$$\begin{aligned} \mathsf{T}_e^{(0)} &= \mathbb{C}_e \xi_{\mathbf{x}} \mathbf{u}^{(0)} + \mathbb{C}_e \xi_{\mathbf{y}} \mathcal{A}_e \xi_{\mathbf{x}} \mathbf{u}^{(0)} + \mathbb{C}_e \xi_{\mathbf{y}} \mathbf{a}_e p_p^{(0)} + \mathbb{C}_e \xi_{\mathbf{y}} \mathbf{b}_e p_{\mathrm{f}}^{(0)} - \hat{\boldsymbol{\alpha}}_e p_p^{(0)} \\ &= (\mathbb{C}_e + \mathbb{C}_e \mathbb{M}_e) \xi_{\mathbf{x}} \mathbf{u}^{(0)} + (\mathbb{C}_e \mathsf{L}_e - \hat{\boldsymbol{\alpha}}_e) p_p^{(0)} + \mathbb{C}_e \mathsf{N}_e p_{\mathrm{f}}^{(0)}, \end{aligned} \tag{68}$$

where we have used the notation for conciseness and readability

$$\mathbb{M}_i = \xi_{\mathbf{y}} \mathcal{A}_i, \quad \mathbb{M}_e = \xi_y \mathcal{A}_e, \quad \mathsf{L}_i = \xi_{\mathbf{y}} \mathbf{a}_i, \quad \mathsf{L}_e = \xi_{\mathbf{y}} \mathbf{a}_e, \quad \mathsf{N}_i = \xi_{\mathbf{y}} \mathbf{b}_i, \quad \text{and} \quad \mathsf{N}_e = \xi_{\mathbf{y}} \mathbf{b}_e. \tag{69}$$

We need a balance equation that takes into consideration the extracellular matrix, the myocyte and the fluid network. Taking the integral average of (41e), (41f) and (41k) gives

$$\int_{\Omega_i} \nabla_{\mathbf{x}} \cdot \mathsf{T}_i^{(0)} \mathrm{d}\mathbf{y} + \int_{\Omega_i} \nabla_{\mathbf{y}} \cdot \mathsf{T}_i^{(1)} \mathrm{d}\mathbf{y} + \int_{\Omega_i} (\mathsf{G}_i \nabla_{\mathbf{x}} \phi_i^{(0)} \times \mathbf{B}^{(0)}) \mathrm{d}\mathbf{y} + \int_{\Omega_i} (\mathsf{G}_i \nabla_{\mathbf{y}} \phi_i^{(1)} \times \mathbf{B}^{(0)}) \mathrm{d}\mathbf{y} + \int_{\Omega_e} \nabla_{\mathbf{x}} \cdot \mathsf{T}_e^{(0)} \mathrm{d}\mathbf{y} + \int_{\Omega_e} \nabla_{\mathbf{y}} \cdot \mathsf{T}_e^{(1)} \mathrm{d}\mathbf{y} + \int_{\Omega_e} (\mathsf{G}_e \nabla_{\mathbf{x}} \phi_e^{(0)} \times \mathbf{B}^{(0)}) \mathrm{d}\mathbf{y}$$
$$+ \int_{\Omega_e} (\mathsf{G}_e \nabla_{\mathbf{y}} \phi_e^{(1)} \times \mathbf{B}^{(0)}) \mathrm{d}\mathbf{y} + \int_{\Omega_{\mathrm{f}}} \nabla_{\mathbf{x}} \cdot \mathsf{T}_{\mathrm{f}}^{(0)} \mathrm{d}\mathbf{y} + \int_{\Omega_{\mathrm{f}}} \nabla_{\mathbf{y}} \cdot \mathsf{T}_{\mathrm{f}}^{(1)} \mathrm{d}\mathbf{y} = 0. \tag{70}$$

We apply the divergence theorem to the second and seventh integral and use the expressions (43a) and (43b) that we have obtained for $\phi_i^{(1)}$ and $\phi_e^{(1)}$ to give

$$\nabla_{\mathbf{x}} \cdot \langle \mathsf{T}_i^{(0)} \rangle_i + \nabla_{\mathbf{x}} \cdot \langle \mathsf{T}_e^{(0)} \rangle_e + \nabla_{\mathbf{x}} \cdot \langle \mathsf{T}_{\mathrm{f}}^{(0)} \rangle_{\mathrm{f}} + \int_{\partial\Omega_i \setminus \Gamma} \mathsf{T}_i^{(1)} \cdot \mathbf{n}_{\partial\Omega_i} \mathrm{d}S - \int_{\Gamma} \mathsf{T}_i^{(1)} \cdot \mathbf{n}_{\Gamma} \mathrm{d}S$$
$$+ \int_{\partial\Omega_e \setminus \Gamma \cup \gamma} \mathsf{T}_e^{(1)} \mathbf{n}_{\partial\Omega_e} \mathrm{d}S + \int_{\Gamma} \mathsf{T}_e^{(1)} \cdot \mathbf{n}_{\Gamma} \mathrm{d}S + \int_{\gamma} \mathsf{T}_e^{(1)} \cdot \mathbf{n}_{\gamma} \mathrm{d}S + \int_{\Omega_i} \mathsf{G}_i \nabla_{\mathbf{x}} \phi_i^{(0)} \times \mathbf{B}^{(0)} \mathrm{d}\mathbf{y}$$
$$+ \int_{\Omega_e} (\mathsf{G}_e \nabla_{\mathbf{x}} \phi_e^{(0)} \times \mathbf{B}^{(0)}) \mathrm{d}\mathbf{y} + \int_{\Omega_i} (\mathsf{G}_i \nabla_{\mathbf{y}} (\boldsymbol{\Phi}_i \nabla_{\mathbf{x}} \phi_i^{(0)} + \hat{\boldsymbol{\Phi}}_i \nabla_{\mathbf{x}} \phi_e^{(0)} + \tilde{\phi}_i) \times \mathbf{B}^{(0)}) \mathrm{d}\mathbf{y}$$
$$+ \int_{\Omega_e} (\mathsf{G}_e \nabla_{\mathbf{y}} (\boldsymbol{\Phi}_e \nabla_{\mathbf{x}} \phi_e^{(0)} + \hat{\boldsymbol{\Phi}}_e \nabla_{\mathbf{x}} \phi_i^{(0)} + \tilde{\phi}_e) \times \mathbf{B}^{(0)}) \mathrm{d}\mathbf{y} + \int_{\partial\Omega_f \setminus \gamma} \mathsf{T}_{\mathrm{f}}^{(1)} \cdot \mathbf{n}_{\partial\Omega_{\mathrm{f}}} \mathrm{d}S - \int_{\gamma} \mathsf{T}_{\mathrm{f}}^{(1)} \cdot \mathbf{n}_{\gamma} \mathrm{d}S = 0. \tag{71}$$

The terms of the external boundaries cancel due to periodicity and the terms on Γ cancel due to (41o) and the terms on γ cancel due to (41u) so that we have

$$\nabla_{\mathbf{x}} \cdot \langle \mathsf{T}_i^{(0)} \rangle_i + \nabla_{\mathbf{x}} \cdot \langle \mathsf{T}_e^{(0)} \rangle_e + \nabla_{\mathbf{x}} \cdot \langle \mathsf{T}_{\mathrm{f}}^{(0)} \rangle_{\mathrm{f}} + \int_{\Omega_i} (\mathsf{G}_i \nabla_{\mathbf{x}} \phi_i^{(0)} \times \mathbf{B}^{(0)}) \mathrm{d}\mathbf{y} + \int_{\Omega_e} (\mathsf{G}_e \nabla_{\mathbf{x}} \phi_e^{(0)} \times \mathbf{B}^{(0)}) \mathrm{d}\mathbf{y}$$
$$+ \int_{\Omega_i} (\mathsf{G}_i \nabla_{\mathbf{y}} \boldsymbol{\Phi}_i \nabla_{\mathbf{x}} \phi_i^{(0)} \times \mathbf{B}^{(0)}) \mathrm{d}\mathbf{y} + \int_{\Omega_i} (\mathsf{G}_i \nabla_{\mathbf{y}} \hat{\boldsymbol{\Phi}}_i \nabla_{\mathbf{x}} \phi_e^{(0)} \times \mathbf{B}^{(0)}) \mathrm{d}\mathbf{y} + \int_{\Omega_i} (\mathsf{G}_i \nabla_{\mathbf{y}} \tilde{\phi}_i \times \mathbf{B}^{(0)}) \mathrm{d}\mathbf{y}$$
$$+ \int_{\Omega_e} (\mathsf{G}_e \nabla_{\mathbf{y}} \boldsymbol{\Phi}_e \nabla_{\mathbf{x}} \phi_e^{(0)} \times \mathbf{B}^{(0)}) \mathrm{d}\mathbf{y} + \int_{\Omega_e} (\mathsf{G}_e \nabla_{\mathbf{y}} \hat{\boldsymbol{\Phi}}_e \nabla_{\mathbf{x}} \phi_i^{(0)} \times \mathbf{B}^{(0)}) \mathrm{d}\mathbf{y} + \int_{\Omega_e} (\mathsf{G}_e \nabla_{\mathbf{y}} \tilde{\phi}_e \times \mathbf{B}^{(0)}) \mathrm{d}\mathbf{y} = 0. \tag{72}$$

We can rewrite by collecting together integrals and using the notation (50) we have

$$\nabla_{\mathbf{x}} \cdot \langle \mathsf{T}_i^{(0)} \rangle_i + \nabla_{\mathbf{x}} \cdot \langle \mathsf{T}_e^{(0)} \rangle_e + \nabla_{\mathbf{x}} \cdot \langle \mathsf{T}_{\mathrm{f}}^{(0)} \rangle_{\mathrm{f}} + \langle \mathsf{G}_i \mathsf{R}_i + \mathsf{G}_i \rangle_i \nabla_{\mathbf{x}} \phi_i^{(0)} \times \langle \mathbf{B}^{(0)} \rangle_i$$
$$+ \langle \mathsf{G}_e \mathsf{R}_e + \mathsf{G}_e \rangle_e \nabla_{\mathbf{x}} \phi_e^{(0)} \times \langle \mathbf{B}^{(0)} \rangle_e + \langle \mathsf{G}_i \mathsf{Q}_i \rangle_i \nabla_{\mathbf{x}} \phi_e^{(0)} \times \langle \mathbf{B}^{(0)} \rangle_i$$
$$+ \langle \mathsf{G}_e \mathsf{Q}_{\mathbf{e}} \rangle_e \nabla_{\mathbf{x}} \phi_i^{(0)} \times \langle \mathbf{B}^{(0)} \rangle_e + \langle \mathsf{G}_i \mathbf{s}_i \times \mathbf{B}^{(0)} \rangle_i + \langle \mathsf{G}_e \mathbf{s}_e \times \mathbf{B}^{(0)} \rangle_e = 0. \tag{73}$$

Which can finally be written as

$$\nabla_{\mathbf{x}} \cdot \langle \mathsf{T}_i^{(0)} \rangle_i + \nabla_{\mathbf{x}} \cdot \langle \mathsf{T}_e^{(0)} \rangle_e = -\langle \mathsf{G}_i \mathsf{R}_i + \mathsf{G}_i \rangle_i \nabla_{\mathbf{x}} \phi_i^{(0)} \times \langle \mathbf{B}^{(0)} \rangle_i - \langle \mathsf{G}_e \mathsf{R}_e + \mathsf{G}_e \rangle_e \nabla_{\mathbf{x}} \phi_e^{(0)} \times \langle \mathbf{B}^{(0)} \rangle_e - \langle \mathsf{G}_i \mathsf{Q}_i \rangle_i \nabla_{\mathbf{x}} \phi_e^{(0)} \times \langle \mathbf{B}^{(0)} \rangle_i - \langle \mathsf{G}_e \mathsf{Q}_{\mathbf{e}} \rangle_e \nabla_{\mathbf{x}} \phi_i^{(0)} \times \langle \mathbf{B}^{(0)} \rangle_e$$
$$- \langle \mathsf{G}_i \mathbf{s}_i \times \mathbf{B}^{(0)} \rangle_i - \langle \mathsf{G}_e \mathbf{s}_e \times \mathbf{B}^{(0)} \rangle_e + \phi \nabla_{\mathbf{x}} p^{(0)}, \tag{74}$$

where we have used $\mathsf{T}_{\mathrm{f}}^{(0)} = -p^{(0)} \mathrm{I}$.

3.6. Problem for vessel fluid flow

We wish to write down a problem for the fluid network flow. We begin with (41n), (33m), (33v) and (33w)

$$\nabla_y^2 \mathbf{v}_{\mathrm{f}}^{(0)} = \nabla_y p_{\mathrm{f}}^{(1)} + \nabla_x p_{\mathrm{f}}^{(0)} \quad \text{in} \quad \Omega_{\mathrm{f}}, \tag{75a}$$
$$\nabla_y \cdot \mathbf{v}_{\mathrm{f}}^{(0)} = 0 \quad \text{in} \quad \Omega_{\mathrm{f}}, \tag{75b}$$
$$(\mathbf{v}_{\mathrm{f}}^{(0)} - \dot{\mathbf{u}}^{(0)}) \cdot \mathbf{n}_{\gamma} = 0 \quad \text{on} \quad \gamma, \tag{75c}$$
$$\tau_\beta \cdot (\mathsf{T}_{\mathrm{f}}^{(1)} \mathbf{n}_{\gamma}) = -\frac{\alpha}{\sqrt{k}} (\mathbf{v}_{\mathrm{f}}^{(0)} - \dot{\mathbf{u}}^{(0)}) \cdot \tau_\beta \quad \text{on} \quad \gamma, \tag{75d}$$

where we have that

$$\mathsf{T}_{\mathrm{f}}^{(1)} = -p_{\mathrm{f}}^{(1)} \mathrm{I} + \xi_{\mathbf{y}}(\mathbf{v}_{\mathrm{f}}^{(0)}). \tag{76}$$

We can define the leading order relative fluid–solid velocity $\mathbf{w}_{\mathrm{f}}^{(0)}$ as

$$\mathbf{w}_{\mathrm{f}}^{(0)} := \mathbf{v}_{\mathrm{f}}^{(0)} - \dot{\mathbf{u}}^{(0)}. \tag{77}$$

Then using this we can write down the problem in terms of the relative-fluid velocity as

$$\nabla_y^2 \mathbf{w}_{\mathrm{f}}^{(0)} - \nabla_y p_{\mathrm{f}}^{(1)} - \nabla_x p_{\mathrm{f}}^{(0)} = 0 \quad \text{in} \quad \Omega_{\mathrm{f}}, \tag{78a}$$
$$\nabla_y \cdot \mathbf{w}_{\mathrm{f}}^{(0)} = 0 \quad \text{in} \quad \Omega_{\mathrm{f}}, \tag{78b}$$
$$\mathbf{w}_{\mathrm{f}}^{(0)} \cdot \mathbf{n}_{\gamma} = 0 \quad \text{on} \quad \gamma, \tag{78c}$$
$$\tau_\beta \cdot (\xi_{\mathbf{y}}(\mathbf{w}_{\mathrm{f}}^{(0)}) \mathbf{n}_{\gamma}) = -\frac{\alpha}{\sqrt{k}} \mathbf{w}_{\mathrm{f}}^{(0)} \cdot \tau_\beta \quad \text{on} \quad \gamma. \tag{78d}$$

We can propose the ansatz

$$\mathbf{w}_{\mathrm{f}}^{(0)} = -\mathsf{W}_{\mathrm{f}} \nabla_x p_{\mathrm{f}}^{(0)}, \tag{79a}$$

$$p_{\mathrm{f}}^{(1)} = -\mathbf{P}_{\mathrm{f}} \cdot \nabla_x p_{\mathrm{f}}^{(0)}. \tag{79b}$$

where W_{f} is a second rank tensor and $\mathbf{P}_{\mathrm{f}}$ is a vector that satisfies

$$\nabla_y^2 \mathsf{W}_{\mathrm{f}}^{\mathrm{T}} = \nabla_y \mathbf{P}_{\mathrm{f}} - \mathrm{I} \quad \text{in} \quad \Omega_{\mathrm{f}}, \tag{80a}$$

$$\nabla_y \cdot \mathsf{W}_{\mathrm{f}}^{\mathrm{T}} = 0 \quad \text{in} \quad \Omega_{\mathrm{f}}, \tag{80b}$$

$$\mathsf{W}_{\mathrm{f}}^{\mathrm{T}} \cdot \mathbf{n}_\gamma = 0 \quad \text{on} \quad \gamma, \tag{80c}$$

$$\tau_\beta \cdot (\xi_{\mathbf{y}}(\mathsf{W}_{\mathrm{f}}^{\mathrm{T}})\mathbf{n}_\gamma) = -\frac{\alpha}{\sqrt{k}} \mathsf{W}_{\mathrm{f}}^{\mathrm{T}} \cdot \tau_\beta \quad \text{on} \quad \gamma, \tag{80d}$$

where periodic conditions apply on the boundary $\partial\Omega_{\mathrm{f}} \setminus \gamma$ and a further condition is to be placed on $\mathbf{P}_{\mathrm{f}}$ for the solution to be unique, such as

$$\langle \mathbf{P}_{\mathrm{f}} \rangle_{\mathrm{f}} = 0. \tag{81}$$

The macroscale flow in the fluid network, which is described in terms of relative fluid–solid velocity, is obtained averaging (79a). That is

$$\langle \mathbf{w}_{\mathrm{f}}^{(0)} \rangle_{\mathrm{f}} = -\langle \mathsf{W}_{\mathrm{f}} \rangle_{\mathrm{f}} \nabla_x p_{\mathrm{f}}^{(0)} \tag{82}$$

The final equation we require governs the fluid pressure. We begin with the incompressibility constraint (41m) and integrate over the fluid domain. That is

$$\int_{\Omega_{\mathrm{f}}} \nabla_{\mathbf{x}} \cdot \mathbf{v}_{\mathrm{f}}^{(0)} \mathrm{d}\mathbf{y} + \int_{\Omega_{\mathrm{f}}} \nabla_{\mathbf{y}} \cdot \mathbf{v}_{\mathrm{f}}^{(1)} \mathrm{d}\mathbf{y} = 0. \tag{83}$$

Which by applying macroscopic uniformity and rearranging can be written as

$$\nabla_{\mathbf{x}} \cdot \langle \mathbf{v}_{\mathrm{f}}^{(0)} \rangle_{\mathrm{f}} + \int_{\Omega_{\mathrm{f}}} \nabla_{\mathbf{y}} \cdot \mathbf{v}_{\mathrm{f}}^{(1)} \mathrm{d}\mathbf{y} = 0. \tag{84}$$

We can then apply the divergence theorem to the integral to obtain

$$\nabla_{\mathbf{x}} \cdot \langle \mathbf{v}_{\mathrm{f}}^{(0)} \rangle_{\mathrm{f}} = -\frac{1}{|\Omega|} \int_\gamma \mathbf{v}_{\mathrm{f}}^{(1)} \cdot \mathbf{n}_\gamma \mathrm{d}S. \tag{85}$$

We want to use the interface condition (41v) to obtain an expression for $\mathbf{v}_{\mathrm{f}}^{(1)} \cdot \mathbf{n}_\gamma$. So we have

$$\mathbf{n}_\gamma \cdot (\mathsf{T}_{\mathrm{f}}^{(0)} \mathbf{n}_\gamma) + \frac{1}{L_p} (\mathbf{v}_{\mathrm{f}}^{(1)} - \dot{\mathbf{u}}_e^{(1)}) \cdot \mathbf{n}_\gamma = -p_p^{(0)} \tag{86}$$

with $\mathsf{T}_{\mathrm{f}}^{(0)} = -p_{\mathrm{f}}^{(0)} \mathrm{I}$, so we can write the interface condition as

$$\mathbf{n}_\gamma \cdot (-p_{\mathrm{f}}^{(0)} \mathbf{n}_\gamma) + \frac{1}{L_p} (\mathbf{v}_{\mathrm{f}}^{(1)} - \dot{\mathbf{u}}_e^{(1)}) \cdot \mathbf{n}_\gamma = -p_p^{(0)}. \tag{87}$$

We can now rearrange this to obtain an expression for $\mathbf{v}^{(1)} \cdot \mathbf{n}_\gamma$ that can be used in the integral (84)

$$-\mathbf{v}_{\mathrm{f}}^{(1)} \cdot \mathbf{n}_\gamma = (p_p^{(0)} - p_{\mathrm{f}}^{(0)}) L_p - \dot{\mathbf{u}}_e^{(1)} \cdot \mathbf{n}_\gamma. \tag{88}$$

We now can rewrite the integral (84) as

$$\nabla_{\mathbf{x}} \cdot \langle \mathbf{v}_{\mathrm{f}}^{(0)} \rangle_{\mathrm{f}} = \frac{1}{|\Omega|} \int_\gamma ((p_p^{(0)} - p_{\mathrm{f}}^{(0)}) L_p - \dot{\mathbf{u}}_e^{(1)} \cdot \mathbf{n}_\gamma) \mathrm{d}S. \tag{89}$$

This becomes

$$\nabla_{\mathbf{x}} \cdot \langle \mathbf{v}_{\mathrm{f}}^{(0)} \rangle_{\mathrm{f}} = \frac{|\gamma| L_p}{|\Omega|} (p_p^{(0)} - p_{\mathrm{f}}^{(0)}) - \frac{1}{|\Omega|} \int_\gamma \dot{\mathbf{u}}_e^{(1)} \cdot \mathbf{n}_\gamma \mathrm{d}S. \tag{90}$$

In order to reverse the divergence theorem on the integral above we must add and subtract the contribution over the solid–solid interface Γ. That is

$$\nabla_{\mathbf{x}} \cdot \langle \mathbf{v}_{\mathrm{f}}^{(0)} \rangle_{\mathrm{f}} = \frac{|\gamma| L_p}{|\Omega|} (p_p^{(0)} - p_{\mathrm{f}}^{(0)}) - \frac{1}{|\Omega|} \int_\gamma \dot{\mathbf{u}}_e^{(1)} \cdot \mathbf{n}_\gamma \mathrm{d}S - \frac{1}{|\Omega|} \int_\Gamma \dot{\mathbf{u}}_e^{(1)} \cdot \mathbf{n}_\Gamma \mathrm{d}S + \frac{1}{|\Omega|} \int_\Gamma \dot{\mathbf{u}}_e^{(1)} \cdot \mathbf{n}_\Gamma \mathrm{d}S. \tag{91}$$

The first two integrals above allow us to reverse the divergence theorem to obtain a term in the extracellular domain, and we can use interface condition (41p) to change the final integral to be in terms of the solid velocity in the myocyte domain

$$\nabla_{\mathbf{x}} \cdot \langle \mathbf{v}_{\mathrm{f}}^{(0)} \rangle_{\mathrm{f}} = \frac{|\gamma| L_p}{|\Omega|} (p_p^{(0)} - p_{\mathrm{f}}^{(0)}) + \frac{1}{|\Omega|} \int_{\Omega_e} \nabla_{\mathbf{y}} \cdot \dot{\mathbf{u}}_e^{(1)} \mathrm{d}\mathbf{y} + \frac{1}{|\Omega|} \int_\Gamma \dot{\mathbf{u}}_i^{(1)} \cdot \mathbf{n}_\Gamma \mathrm{d}S. \tag{92}$$

Since the myocyte domain has entire boundary Γ we can then reverse the divergence theorem on the final integral to obtain

$$\nabla_{\mathbf{x}} \cdot \langle \mathbf{v}_{\mathrm{f}}^{(0)} \rangle_{\mathrm{f}} = \frac{|\gamma| L_p}{|\Omega|} (p_p^{(0)} - p_{\mathrm{f}}^{(0)}) + \frac{1}{|\Omega|} \int_{\Omega_e} \nabla_{\mathbf{y}} \cdot \dot{\mathbf{u}}_e^{(1)} \mathrm{d}\mathbf{y} + \frac{1}{|\Omega|} \int_{\Omega_i} \nabla_{\mathbf{y}} \cdot \dot{\mathbf{u}}_i^{(1)} \mathrm{d}\mathbf{y}. \tag{93}$$

This can be written as

$$\nabla_{\mathbf{x}} \cdot \langle \mathbf{v}_{\mathrm{f}}^{(0)} \rangle_{\mathrm{f}} = \frac{|\gamma| L_p}{|\Omega|} (p^{(0)} - p_{\mathrm{f}}^{(0)}) + \langle \nabla_{\mathbf{y}} \cdot \dot{\mathbf{u}}_e^{(1)} \rangle_e + \langle \nabla_{\mathbf{y}} \cdot \dot{\mathbf{u}}_i^{(1)} \rangle_i. \tag{94}$$

Or indeed as

$$\nabla_{\mathbf{x}} \cdot \langle \mathbf{v}_{\mathrm{f}}^{(0)} \rangle_{\mathrm{f}} = \frac{|\gamma| L_p}{|\Omega|} (p_p^{(0)} - p_{\mathrm{f}}^{(0)}) + \langle \mathrm{Tr}(\xi_{\mathbf{y}} \dot{\mathbf{u}}_e^{(1)}) \rangle_e + \langle \mathrm{Tr}(\xi_{\mathbf{y}} \dot{\mathbf{u}}_i^{(1)}) \rangle_i. \tag{95}$$

Since we have expressions for $\mathbf{u}_i^{(1)}$ and $\mathbf{u}_e^{(1)}$ (62a) and (62b) we can write the relationship as

$$\begin{aligned} \nabla_{\mathbf{x}} \cdot \langle \mathbf{v}_{\mathrm{f}}^{(0)} \rangle_{\mathrm{f}} = {} & \frac{|\gamma| L_p}{|\Omega|} (p_p^{(0)} - p_{\mathrm{f}}^{(0)}) + \langle \mathrm{Tr}(\xi_{\mathbf{y}} \mathcal{A}_e) \rangle_e \xi_{\mathbf{x}} \dot{\mathbf{u}}^{(0)} + \langle \mathrm{Tr}(\xi_{\mathbf{y}} \mathbf{a}_e) \rangle_e \dot{p}_p^{(0)} \\ & + \langle \mathrm{Tr}(\xi_{\mathbf{y}} \mathbf{b}_e) \rangle_e \dot{p}_{\mathrm{f}}^{(0)} + \langle \mathrm{Tr}(\xi_{\mathbf{y}} \mathcal{A}_i) \rangle_i \xi_{\mathbf{x}} \dot{\mathbf{u}}^{(0)} + \langle \mathrm{Tr}(\xi_{\mathbf{y}} \mathbf{a}_i) \rangle_i \dot{p}_p^{(0)} + \langle \mathrm{Tr}(\xi_{\mathbf{y}} \mathbf{b}_i) \rangle_i \dot{p}_{\mathrm{f}}^{(0)} \end{aligned} \tag{96}$$

Using the notation we defined in (69) we have

$$\nabla_{\mathbf{x}} \cdot \langle \mathbf{v}_{\mathrm{f}}^{(0)} \rangle_{\mathrm{f}} = \frac{|\gamma| L_p}{|\Omega|} (p_p^{(0)} - p_{\mathrm{f}}^{(0)}) + (\langle \mathrm{Tr}\mathbb{M}_e \rangle_e + \langle \mathrm{Tr}\mathbb{M}_i \rangle_i) \xi_{\mathbf{x}} \dot{\mathbf{u}}^{(0)} + (\langle \mathrm{Tr}\mathsf{L}_i \rangle_i + \langle \mathrm{Tr}\mathsf{L}_e \rangle_e) \dot{p}_p^{(0)} + (\langle \mathrm{Tr}\mathsf{N}_i \rangle_i + \langle \mathrm{Tr}\mathsf{N}_e \rangle_e) \dot{p}_{\mathrm{f}}^{(0)}. \tag{97}$$

We recall that we have the expression for the relative fluid–solid velocity $\mathbf{w}_{\mathrm{f}} = \mathbf{v}_{\mathrm{f}}^{(0)} - \dot{\mathbf{u}}^{(0)}$. This can be rearranged for $\mathbf{v}_{\mathrm{f}}^{(0)}$ and substituted in (97) to obtain

$$\nabla_{\mathbf{x}} \cdot (\langle \mathbf{w}_{\mathrm{f}}^{(0)} \rangle_{\mathrm{f}} + \phi \dot{\mathbf{u}}^{(0)}) = \frac{|\gamma| L_P}{|\Omega|} (p_p^{(0)} - p_{\mathrm{f}}^{(0)}) + (\langle \mathrm{Tr}\mathbb{M}_e \rangle_e + \langle \mathrm{Tr}\mathbb{M}_i \rangle_i) \xi_{\mathbf{x}} \dot{\mathbf{u}}^{(0)} + (\langle \mathrm{Tr}\mathsf{L}_i \rangle_i + \langle \mathrm{Tr}\mathsf{L}_e \rangle_e) \dot{p}_p^{(0)} + (\langle \mathrm{Tr}\mathsf{N}_i \rangle_i + \langle \mathrm{Tr}\mathsf{N}_e \rangle_e) \dot{p}_{\mathrm{f}}^{(0)}. \tag{98}$$

We can expand the left hand side of (98) and note that we are able to express $\phi \nabla_{\mathbf{x}} \cdot \dot{\mathbf{u}}^{(0)}$ as $\phi \mathrm{I} : \xi_{\mathbf{x}} \dot{\mathbf{u}}^{(0)}$ to obtain

$$\nabla_{\mathbf{x}} \cdot \langle \mathbf{w}_{\mathrm{f}}^{(0)} \rangle_{\mathrm{f}} = \frac{|\gamma| L_p}{|\Omega|} (p_p^{(0)} - p_{\mathrm{f}}^{(0)}) + (\langle \mathrm{Tr}\mathbb{M}_e \rangle_e + \langle \mathrm{Tr}\mathbb{M}_i \rangle_i - \phi \mathrm{I}) : \xi_{\mathbf{x}} \dot{\mathbf{u}}^{(0)} + (\langle \mathrm{Tr}\mathsf{L}_i \rangle_i + \langle \mathrm{Tr}\mathsf{L}_e \rangle_e) \dot{p}_p^{(0)} + (\langle \mathrm{Tr}\mathsf{N}_i \rangle_i + \langle \mathrm{Tr}\mathsf{N}_e \rangle_e) \dot{p}_{\mathrm{f}}^{(0)}. \tag{99}$$

3.7. Problem for interstitial flow

We wish to write down a problem for the interstitial fluid flow. We begin with (33j), (41s) and (41t)

$$\nabla_{\mathbf{y}} \cdot \mathbf{w}_e^{(0)} = 0 \qquad \text{in} \quad \Omega_e \tag{100a}$$

$$\mathbf{w}_e^{(0)} \cdot \mathbf{n}_\gamma = \mathbf{w}_{\mathrm{f}}^{(0)} \cdot \mathbf{n}_\gamma \qquad \text{on} \quad \gamma \tag{100b}$$

$$\mathbf{w}_e^{(0)} \cdot \mathbf{n}_\Gamma = 0 \qquad \text{on} \quad \Gamma \tag{100c}$$

We can use (41i), the definition that $\mathbf{w}_{\mathrm{f}}^{(0)} = \mathbf{v}_{\mathrm{f}}^{(0)} - \dot{\mathbf{u}}^{(0)}$ and (33v) to rewrite the problem as

$$\nabla_{\mathbf{y}} \cdot (\mathsf{K}_e \nabla_{\mathbf{y}} p_p^{(1)}) = -\nabla_{\mathbf{y}} \cdot (\mathsf{K}_e \nabla_{\mathbf{x}} p_p^{(0)}) \qquad \text{in} \quad \Omega_e \tag{101a}$$

$$(\mathsf{K}_e \nabla_{\mathbf{y}} p_p^{(1)}) \cdot \mathbf{n}_\gamma = -(\mathsf{K}_e \nabla_{\mathbf{x}} p_p^{(0)}) \cdot \mathbf{n}_\gamma \qquad \text{on} \quad \gamma \tag{101b}$$

$$(\mathsf{K}_e \nabla_{\mathbf{y}} p_p^{(1)}) \cdot \mathbf{n}_\Gamma = -(\mathsf{K}_e \nabla_{\mathbf{x}} p_p^{(0)}) \cdot \mathbf{n}_\Gamma \qquad \text{on} \quad \Gamma \tag{101c}$$

We can propose the ansatz

$$p_p^{(1)} = -\mathbf{P}_p \cdot \nabla_{\mathbf{x}} p_p^{(0)} \tag{102}$$

where $\mathbf{P}_p$ is a vector that satisfies the following cell problem

$$\nabla_{\mathbf{y}} \cdot (\nabla_{\mathbf{y}} \mathbf{P}_p \mathsf{K}_e^{\mathrm{T}}) = -\nabla_{\mathbf{y}} \cdot \mathsf{K}_e^{\mathrm{T}} \qquad \text{in} \quad \Omega_e \tag{103a}$$

$$(\nabla_{\mathbf{y}} \mathbf{P}_p \mathsf{K}_e^{\mathrm{T}}) \cdot \mathbf{n}_\gamma = -\mathsf{K}_e^{\mathrm{T}} \cdot \mathbf{n}_\gamma \qquad \text{on} \quad \gamma \tag{103b}$$

$$(\nabla_{\mathbf{y}} \mathbf{P}_p \mathsf{K}_e^{\mathrm{T}}) \cdot \mathbf{n}_\Gamma = -\mathsf{K}_e^{\mathrm{T}} \cdot \mathbf{n}_\Gamma \qquad \text{on} \quad \Gamma \tag{103c}$$

where periodic conditions apply on the boundary $\partial\Omega \setminus \Gamma \cup \gamma$ and a further condition is to be placed on the auxiliary vectors for the solution to be unique, such as

$$\langle \mathbf{P}_p \rangle_e = 0 \tag{104}$$

We can now write the leading order Darcy's law in the extracellular domain using the ansatz. That is,

$$\langle \mathbf{w}_e^{(0)} \rangle_e = \langle \mathsf{K}_e (\nabla_{\mathbf{y}} \mathbf{P}_p)^{\mathrm{T}} - \mathsf{K}_e \rangle_e \nabla_{\mathbf{x}} p_p^{(0)} \tag{105}$$

We require one final equation to describe the interstitial fluid flow. We begin with (41j) which is given by

$$\frac{\dot{p}_p^{(0)}}{\mathcal{M}_e} = -\hat{\boldsymbol{\alpha}}_e : \xi_y \dot{\mathbf{u}}_e^{(1)} - \hat{\boldsymbol{\alpha}}_e : \xi_x \dot{\mathbf{u}}^{(0)} - \nabla_y \cdot \mathbf{w}_e^{(1)} - \nabla_x \cdot \mathbf{w}_e^{(0)}, \tag{106}$$

we now rearrange and apply the integral average to obtain

$$\nabla_x \cdot \langle \mathbf{w}_e^{(0)} \rangle_e = -\phi_e \frac{\dot{p}_p^{(0)}}{\mathcal{M}_e} - \langle \hat{\boldsymbol{\alpha}}_e : \xi_y \dot{\mathbf{u}}_e^{(1)} \rangle_e - \langle \hat{\boldsymbol{\alpha}}_e \rangle_e : \xi_x \dot{\mathbf{u}}^{(0)} - \frac{1}{|\Omega|} \int_{\Omega_e} \nabla_y \cdot \mathbf{w}_e^{(1)} \mathrm{d}\mathbf{y}. \tag{107}$$

We can then apply the divergence theorem to the integral in (107) to obtain

$$\nabla_x \cdot \langle \mathbf{w}_e^{(0)} \rangle_e = -\phi_e \frac{\dot{p}_p^{(0)}}{\mathcal{M}_e} - \langle \hat{\boldsymbol{\alpha}}_e : \xi_y \dot{\mathbf{u}}_e^{(1)} \rangle_e - \langle \hat{\boldsymbol{\alpha}}_e \rangle_e : \xi_x \dot{\mathbf{u}}^{(0)} - \frac{1}{|\Omega|} \int_\Gamma \mathbf{w}_e^{(1)} \cdot \mathbf{n}_\Gamma \mathrm{dS} - \frac{1}{|\Omega|} \int_\gamma \mathbf{w}_e^{(1)} \cdot \mathbf{n}_\gamma \mathrm{dS}, \tag{108}$$

Since we have the interface conditions (41s) and (41t), we can use these to rewrite the two integrals as

$$\nabla_x \cdot \langle \mathbf{w}_e^{(0)} \rangle_e = -\phi_e \frac{\dot{p}_p^{(0)}}{\mathcal{M}_e} - \langle \hat{\boldsymbol{\alpha}}_e : \xi_y \dot{\mathbf{u}}_e^{(1)} \rangle_e - \langle \hat{\boldsymbol{\alpha}}_e \rangle_e : \xi_x \dot{\mathbf{u}}^{(0)} - \frac{1}{|\Omega|} \int_\Gamma 0 \mathrm{dS} - \frac{1}{|\Omega|} \int_\gamma \mathbf{w}_{\mathrm{f}}^{(1)} \cdot \mathbf{n}_\gamma \mathrm{dS}, \tag{109}$$

We also have Eq. (41v), with (33m) which allows us to write $\mathbf{w}_{\mathrm{f}}^{(1)} \cdot \mathbf{n}_\gamma$ as

$$\mathbf{w}_{\mathrm{f}}^{(1)} \cdot \mathbf{n}_\gamma = -L_p (p_p^{(0)} - p_{\mathrm{f}}^{(0)}) \tag{110}$$

and therefore we can use this in the final integral and rewrite the expression as

$$\nabla_x \cdot \langle \mathbf{w}_e^{(0)} \rangle_e = -\phi_e \frac{\dot{p}_p^{(0)}}{\mathcal{M}_e} - \langle \hat{\boldsymbol{\alpha}}_e : \xi_y \dot{\mathbf{u}}_e^{(1)} \rangle_e - \langle \hat{\boldsymbol{\alpha}}_e \rangle_e : \xi_x \dot{\mathbf{u}}^{(0)} - \frac{1}{|\Omega|} \int_\Gamma 0 \mathrm{dS} + \frac{|\gamma| L_p}{|\Omega|} (p_p^{(0)} - p_{\mathrm{f}}^{(0)}) \tag{111}$$

We can reverse the divergence theorem on the remaining integral to obtain

$$\nabla_x \cdot \langle \mathbf{w}_e^{(0)} \rangle_e = -\phi_e \frac{\dot{p}_p^{(0)}}{\mathcal{M}_e} - \langle \hat{\boldsymbol{\alpha}}_e : \xi_y \dot{\mathbf{u}}_e^{(1)} \rangle_e - \langle \hat{\boldsymbol{\alpha}}_e \rangle_e : \xi_x \dot{\mathbf{u}}^{(0)} + \frac{|\gamma| L_p}{|\Omega|} (p_p^{(0)} - p_{\mathrm{f}}^{(0)}), \tag{112}$$

We are able to use the expression that we have for $\dot{\mathbf{u}}_e^{(1)}$ (62b) to obtain

$$\nabla_x \cdot \langle \mathbf{w}_e^{(0)} \rangle_e = \langle \mathbb{M}_e^{\mathrm{T}} : \hat{\boldsymbol{\alpha}}_e - \hat{\boldsymbol{\alpha}}_e \rangle_e : \xi_{\mathbf{x}} \dot{\mathbf{u}}^{(0)} - \langle \hat{\boldsymbol{\alpha}}_e : \mathsf{L}_e \rangle_e \dot{p}_p^{(0)} - \langle \hat{\boldsymbol{\alpha}}_e : \mathsf{N}_e \rangle_e \dot{p}_{\mathrm{f}}^{(0)} - \phi_e \frac{\dot{p}_p^{(0)}}{\mathcal{M}_e} + \frac{|\gamma| L_p}{|\Omega|} (p_p^{(0)} - p_{\mathrm{f}}^{(0)}). \tag{113}$$

We have now derived our complete macroscale model for the electrical activity and mechanical deformations in the perfused myocardium.

4. Macroscale model

The macroscale governing equations describe the effective homogenised behaviour of the myocardium in terms of the leading order elastic displacement $\mathbf{u}^{(0)}$, the leading order electric potentials $\phi_i^{(0)}$ and $\phi_e^{(0)}$, the relative fluid solid velocities $\mathbf{w}_{\mathrm{f}}^{(0)}$ and $\mathbf{w}_e^{(0)}$ and the pressures $p_p^{(0)}$ and $p_f^{(0)}$. Our model in the homogenised domain Ω_H is given by

$$\nabla_{\mathbf{x}} \cdot \langle \mathbf{j}_i^{(0)} \rangle_i + \nabla_{\mathbf{x}} \cdot \langle \mathbf{j}_e^{(0)} \rangle_e = \hat{\beta} V^{(0)} (|\Omega_e| - |\Omega_i|) - |\Omega_e| I_i - |\Omega_i| I_e, \tag{114a}$$

$$\begin{aligned} \nabla_{\mathbf{x}} \cdot \langle \mathsf{T}_i^{(0)} \rangle_i + \nabla_{\mathbf{x}} \cdot \langle \mathsf{T}_e^{(0)} \rangle_e = &-\langle \mathsf{G}_i \mathsf{R}_i + \mathsf{G}_i \rangle_i \nabla_{\mathbf{x}} \phi_i^{(0)} \times \langle \mathbf{B}^{(0)} \rangle_i - \langle \mathsf{G}_e \mathsf{R}_e + \mathsf{G}_e \rangle_e \nabla_{\mathbf{x}} \phi_e^{(0)} \times \langle \mathbf{B}^{(0)} \rangle_e - \langle \mathsf{G}_i \mathsf{Q}_i \rangle_i \nabla_{\mathbf{x}} \phi_e^{(0)} \times \langle \mathbf{B}^{(0)} \rangle_i - \langle \mathsf{G}_e \mathsf{Q}_e \rangle_e \nabla_{\mathbf{x}} \phi_i^{(0)} \times \langle \mathbf{B}^{(0)} \rangle_e \\ &- \langle \mathsf{G}_i \mathbf{s}_i \times \mathbf{B}^{(0)} \rangle_i - \langle \mathsf{G}_e \mathbf{s}_e \times \mathbf{B}^{(0)} \rangle_e + \phi \nabla_{\mathbf{x}} p^{(0)}, \end{aligned} \tag{114b}$$

$$\phi_i^{(0)} - \phi_e^{(0)} = V^{(0)}, \tag{114c}$$

$$\nabla_{\mathbf{x}} \cdot \langle \mathbf{w}_{\mathrm{f}}^{(0)} \rangle_{\mathrm{f}} = \frac{|\gamma| L_p}{|\Omega|} (p_p^{(0)} - p_{\mathrm{f}}^{(0)}) + (\langle \mathrm{Tr} \mathbb{M}_e \rangle_e + \langle \mathrm{Tr} \mathbb{M}_i \rangle_i - \phi \mathrm{I}) : \xi_{\mathbf{x}} \dot{\mathbf{u}}^{(0)} + (\langle \mathrm{Tr} \mathsf{L}_i \rangle_i + \langle \mathrm{Tr} \mathsf{L}_e \rangle_e) \dot{p}_p^{(0)} + (\langle \mathrm{Tr} \mathsf{N}_i \rangle_i + \langle \mathrm{Tr} \mathsf{N}_e \rangle_e) \dot{p}_{\mathrm{f}}^{(0)}. \tag{114d}$$

$$\nabla_x \cdot \langle \mathbf{w}_e^{(0)} \rangle_e = \langle \mathbb{M}_e^{\mathrm{T}} : \hat{\boldsymbol{\alpha}}_e - \hat{\boldsymbol{\alpha}}_e \rangle_e : \xi_{\mathbf{x}} \dot{\mathbf{u}}^{(0)} - \langle \hat{\boldsymbol{\alpha}}_e : \mathsf{L}_e \rangle_e \dot{p}_p^{(0)} - \langle \hat{\boldsymbol{\alpha}}_e : \mathsf{N}_e \rangle_e \dot{p}_{\mathrm{f}}^{(0)} - \phi_e \frac{\dot{p}_p^{(0)}}{\mathcal{M}_e} + \frac{|\gamma| L_p}{|\Omega|} (p_p^{(0)} - p_{\mathrm{f}}^{(0)}) \tag{114e}$$

where we have the averaged leading order current densities

$$\langle \mathbf{j}_i^{(0)} \rangle_i = -\langle \mathsf{G}_i + \mathsf{G}_i \mathsf{R}_i \rangle_i \nabla_{\mathbf{x}} \phi_i^{(0)} - \langle \mathsf{G}_i \mathsf{Q}_i \rangle_i \nabla_{\mathbf{x}} \phi_e^{(0)} - \langle \mathsf{G}_i \mathbf{s}_i \rangle_i \tag{115a}$$

$$\langle \mathbf{j}_e^{(0)} \rangle_e = -\langle \mathsf{G}_e + \mathsf{G}_e \mathsf{R}_e \rangle_e \nabla_{\mathbf{x}} \phi_e^{(0)} - \langle \mathsf{G}_e \mathsf{Q}_e \rangle_e \nabla_{\mathbf{x}} \phi_i^{(0)} - \langle \mathsf{G}_e \mathbf{s}_e \rangle_e \tag{115b}$$

and the averaged leading order solid stresses

$$\langle \mathsf{T}_i^{(0)} \rangle_i = \langle \mathbb{C}_i + \mathbb{C}_i \mathbb{M}_i \rangle_i \xi_{\mathbf{x}} \mathbf{u}^{(0)} + \langle \mathbb{C}_i \mathsf{L}_i \rangle_i p_p^{(0)} + \langle \mathbb{C}_i \mathsf{N}_i \rangle_i p_{\mathrm{f}}^{(0)} \tag{116a}$$

$$\langle \mathsf{T}_e^{(0)} \rangle_i = \langle \mathbb{C}_e + \mathbb{C}_e \mathbb{M}_e \rangle_e \xi_{\mathbf{x}} \mathbf{u}^{(0)} + \langle \mathbb{C}_e \mathsf{L}_e - \hat{\boldsymbol{\alpha}}_e \rangle_e p_p^{(0)} + \langle \mathbb{C}_e \mathsf{N}_e \rangle_e p_{\mathrm{f}}^{(0)} \tag{116b}$$

and finally the leading order relative fluid–solid velocities are

$$\langle \mathbf{w}_{\mathrm{f}}^{(0)} \rangle_{\mathrm{f}} = -\langle \mathsf{W}_{\mathrm{f}} \rangle_{\mathrm{f}} \nabla_x p_{\mathrm{f}}^{(0)} \tag{117a}$$

$$\langle \mathbf{w}_e^{(0)} \rangle_e = \langle \mathsf{K}_e (\nabla_{\mathbf{y}} \mathbf{P}_p)^{\mathrm{T}} - \mathsf{K}_e \rangle_e \nabla_{\mathbf{x}} p_p^{(0)} \tag{117b}$$

The novel model comprises the balance equation for the leading order current densities (114a). The current densities (115a) and (115b) comprise both the electric fields of each compartment premultiplied by second rank tensors that are to be obtained by solving the cell problems (44a)–(44e) and (45a)–(45e) and a vector term that arises from premultiplying the solutions to the cell problem (46a)–(46e) by the conductivity tensors. These coefficients arising from the cell problem solutions account for the differences in the electric potentials in each phase and encode these in the model.

To solve the homogenised model (114a)–(114e) in Ω_H it must be supplemented by external boundary conditions on $\partial\Omega_H$ and initial conditions for the macroscale solid displacement, potentials, pressures and relative fluid–solid velocities are required.

We can re-write the balance as follows when using (63a) and (63b)

$$\nabla_{\mathbf{x}} \cdot \left(\left(\langle \mathsf{G}_i + \mathsf{G}_i \mathsf{R}_i \rangle_i + \langle \mathsf{G}_e \mathsf{Q}_e \rangle_e \right) \nabla_{\mathbf{x}} \phi_i^{(0)} + \left(\langle \mathsf{G}_e + \mathsf{G}_e \mathsf{R}_e \rangle_e + \langle \mathsf{G}_i \mathsf{Q}_i \rangle_i \right) \nabla_{\mathbf{x}} \phi_e^{(0)} + \left(\langle \mathsf{G}_i \mathbf{s}_i \rangle_i + \langle \mathsf{G}_e \mathbf{s}_e \rangle_e \right) \right) = \hat{\beta} V^{(0)} (|\Omega_e| - |\Omega_i|) - |\Omega_e| I_i - |\Omega_i| I_e, \tag{118}$$

The Eq. (114c) provides a constraint such that the $V^{(0)}$ is a given and therefore allows that only one of $\phi_i^{(0)}$ or $\phi_e^{(0)}$ is to be calculated in order to obtain both. We can substitute (61e) written in the form $\phi_i^{(0)} = \phi_e^{(0)} + V^{(0)}$ into (118) and rearrange to obtain

$$\nabla_{\mathbf{x}}\cdot\left(\left(\langle \mathsf{G}_i+\mathsf{G}_i\mathsf{R}_i\rangle_i+\langle \mathsf{G}_e\mathsf{Q}_e\rangle_e+\langle \mathsf{G}_e+\mathsf{G}_e\mathsf{R}_e\rangle_e+\langle \mathsf{G}_i\mathsf{Q}_i\rangle_i\right)\nabla_{\mathbf{x}}\phi_e^{(0)}\right)$$
$$=\nabla_{\mathbf{x}}\cdot\left(-\left(\langle \mathsf{G}_i+\mathsf{G}_i\mathsf{R}_i\rangle_i+\langle \mathsf{G}_e\mathsf{Q}_e\rangle_e\right)\nabla_{\mathbf{x}}V^{(0)}-\langle \mathsf{G}_i\mathbf{s}_i\rangle_i-\langle \mathsf{G}_e\mathbf{s}_e\rangle_e\right)+\hat{\beta}V^{(0)}(|\Omega_e|-|\Omega_i|)-|\Omega_e|I_i-|\Omega_i|I_e, \tag{119}$$

We can define the following

$$\mathsf{D}:=\langle \mathsf{G}_i+\mathsf{G}_i\mathsf{R}_i\rangle_i+\langle \mathsf{G}_e\mathsf{Q}_e\rangle_e+\langle \mathsf{G}_e+\mathsf{G}_e\mathsf{R}_e\rangle_e+\langle \mathsf{G}_i\mathsf{Q}_i\rangle_i, \tag{120}$$
$$\mathbf{f}:=-\left(\langle \mathsf{G}_i+\mathsf{G}_i\mathsf{R}_i\rangle_i+\langle \mathsf{G}_e\mathsf{Q}_e\rangle_e\right)\nabla_{\mathbf{x}}V^{(0)}-\langle \mathsf{G}_i\mathbf{s}_i\rangle_i-\langle \mathsf{G}_e\mathbf{s}_e\rangle_e, \tag{121}$$
$$\tilde{\beta}=\hat{\beta}(|\Omega_e|-|\Omega_i|), \tag{122}$$

and therefore (119) can be written as

$$\nabla_{\mathbf{x}}\cdot\left(\mathsf{D}\nabla_{\mathbf{x}}\phi_e^{(0)}\right)=\nabla_{\mathbf{x}}\cdot\mathbf{f}-\tilde{\beta}V^{(0)}-|\Omega_e|I_i-|\Omega_i|I_e. \tag{123}$$

We also have the balance equation for the solid stresses (114b), where the stresses are (116a)–(116b). These stresses comprise tensors $\mathbb{C}_i+\mathbb{C}_i\mathbb{M}_i$ and $\mathbb{C}_e+\mathbb{C}_e\mathbb{M}_e$ which are to be found by solving (63a)–(63e). The stresses also contain terms relating to the interstitial pressure and the fluid pressure where the coefficients of these terms are to be found by solving (64a)–(64e) and (65a)–(65e). The problems to be solved are similar to those found for elastic composite in Penta and Gerisch (2015) and Penta and Gerisch (2017a), poroelastic composites in Miller and Penta (2020, 2022b) and Miller and Penta (2022a) and double poroelastic (Miller and Penta, 2021a). The balance Eq. (114b) also has terms that show the influence of the electric potentials and Lorentz forces on the deformations of the material. These terms again arise by solving the cell problems (44a)–(44e) and (45a)–(45e) and (46a)–(46e).

The final two Eqs. (114d) and (114e) represent the balance of the relative fluid–solid velocities of the vessels and interstitial fluid. These relative fluid–solid velocities are given by (117a) and (117b) where the coefficients are to be obtained by solving (80a)–(80d) and (103a)–(103c) We see that these are related to the strains of the elastic myocyte and the poroelastic extracellular matrix and to the fluid transport between the compartments due to the leakage of the fluid from the vessels into the poroelastic matrix.

5. Numerical example — electrical conductance of the perfused myocardium

In this section we wish to consider a first example of what our novel model can tell us about the electrical conductivity of the myocardium. We consider the macroscale balance Eq. (123), restated here for convenience. We have

$$\nabla_{\mathbf{x}}\cdot\left(\mathsf{D}\nabla_{\mathbf{x}}\phi_e^{(0)}\right)=\nabla_{\mathbf{x}}\cdot\mathbf{f}-\tilde{\beta}V^{(0)}-|\Omega_e|I_i-|\Omega_i|I_e. \tag{124}$$

The cell problems (44a)–(44e) and (45a)–(45e) can be solved to determine the second rank tensor D which we call the effective conductance tensor as well as the vector $\mathbf{f}$. We take this opportunity to study the tensor D in the case of modelling the electrical, vascularised myocardium.

We are considering the effective conductance tensor of the myocardium and we wish to consider it post myocardial infarction. In this case, physiologically it can be observed that the volume fraction of myocytes in the infarct zone decreases due to the death and damage of myocytes. This dramatically reduces the functionality of the heart and therefore the heart looks for a way to regain homeostasis. So for this reason in the regions surrounding the infarct zone the intact myocytes increase in volume to attempt to compensate for the section of damaged heart (Olivetti et al., 1987). We wish to consider the effect that the change in volume has on the electrical conductivity of the myocardium. We should note that we are assuming that the increases in myocyte volume fraction that we are studying correspond to different infarct sizes (and therefore the greater the infarct the greater the increase in the healthy myocytes to compensate) and not a time dependent increase following the infarction (Olivetti et al., 1994; Anversa et al., 1985).

As the 3D geometry of our unit cell is assumed to be a cube with cylindrical myocyte extending in the z-axis direction, as well as 4 vessels (one in each corner of the cube) also extending in the direction of the z-axis we are able to cut the plane and carry out 2D simulations which will be less computationally expensive whilst still retaining the desired accuracy, see Parnell and Abrahams (2006, 2008) and Miller and Penta (2022a) for a reduction of poroelastic type cell problems from 3D to 2D and validation of the 2D simulations. The cell problems are therefore to be solved on the following 2D composite geometry Fig. 2. We use the following conductivity tensors obtained from Roth (1991) and Sachse et al. (2009) for the transversal and longitudinal conductivities in the myocyte and extracellular matrix

$$\mathsf{G}_i=\begin{pmatrix}0.047 & 0\\ 0 & 0.469\end{pmatrix},\quad\text{and}\quad \mathsf{G}_e=\begin{pmatrix}0.214 & 0\\ 0 & 0.375\end{pmatrix}. \tag{125}$$

We now present the results for the conductance tensor D in the transversal and longitudinal directions. We consider the two components of the second rank tensor D in the balance Eq. (123). From Fig. 3(a) we can see the effective conductivity decreases in the transversal direction with the increasing myocyte volume. We can explain this due to the fact that the myocyte has a much lower conductivity in the transversal direction than the extracellular matrix therefore as the volume of the myocyte increases the homogenised effective conductivity tensor D then the influence of the low transversal conductance creates a decrease in the transversal conductance. In Fig. 3(b) we can see that the longitudinal effective conductivity increases with increasing myocyte volume. This can be explained due to the fact that the myocyte has already a higher longitudinal conductance that the extracellular matrix and is it increases in volume this larger value plays an increasingly important role in the conductance of D. The myocytes in adjacent cells join end to end therefore the larger the volume fraction of the myocyte the larger the contact area between adjacent myocytes leading to the increasing longitudinal conductance.

We now carry out the simulations to investigate the influence that on the conductance at four fixed fluid volume fractions $\phi_f=5\%,10\%,15\%,20\%$ and for each of these varying the myocyte volume fraction from 5–40%. The fluid volume fractions have been chosen to represent the following settings; 5% reduced flow leading to infarction, 10–15% normal range of healthy perfusion, 20% over perfused leading to myocardial injury.

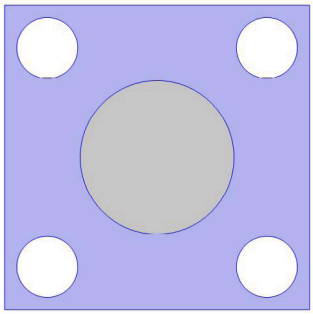

Fig. 2. The Comsol Multiphysics geometry for the electrical cell problems.

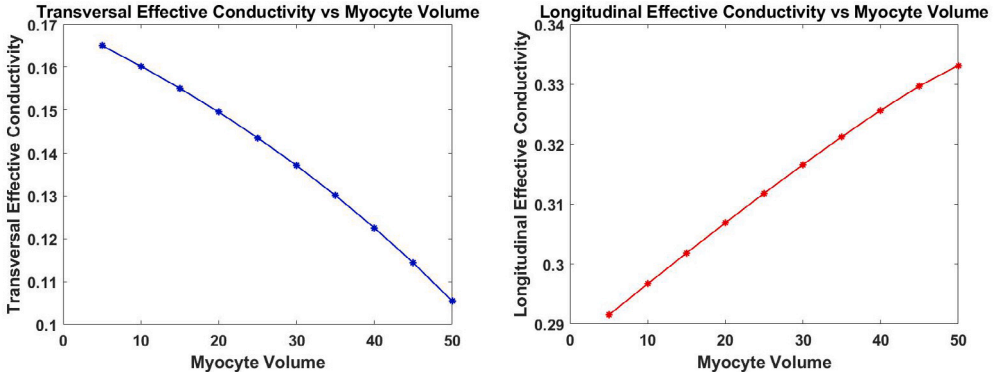

(a) Transversal conductivity vs myocyte volume (b) Longitudinal conductivity vs myocyte volume

Fig. 3. Plots of the components of the second rank effective conductivity tensor D.

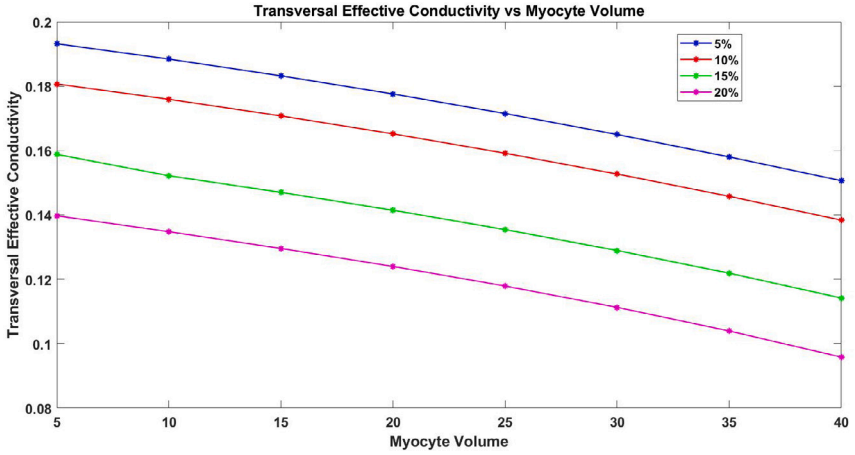

Fig. 4. The transverse conductance vs myocyte volume for four fixed fluid volume fractions.

In figure Fig. 4 we can see that the effective conductivity decreases in the transversal direction with the increasing myocyte volume for all four fixed fluid volume fractions. We see the conductivity value decreases with increasing fluid volume fraction. We can explain this due to the fact that the myocyte has a much lower conductivity in the transversal direction than the extracellular matrix. Therefore as the volume of the myocyte increases and indeed as we consider a matrix with larger vessels (increasing fluid volume fraction) the homogenised effective conductivity tensor D will show the decrease due to the fact that the extracellular matrix which has the higher transversal conductance is getting taken over by the myocyte and the vessels which have lower and zero conductance respectively. Thus meaning that we have a decrease in the transversal conductance.

In figure Fig. 5 we can see that the longitudinal effective conductivity increases with increasing myocyte volume for all four fixed fluid volume fractions. We see that the longitudinal conductivity value is lower the higher the fluid volume fraction. The behaviour here can be explained due to the fact that the myocyte has already a higher longitudinal conductance than the extracellular matrix and as it increases in volume this larger value plays an increasingly important role in the conductance of D. The increasing fluid volume causes the transversal conductance to become lower as we have a larger vessel volume and these have zero conductance. The myocytes in adjacent cells join end to end therefore the larger the volume fraction of the myocyte the larger the contact area between adjacent myocytes leading to the increasing longitudinal conductance.

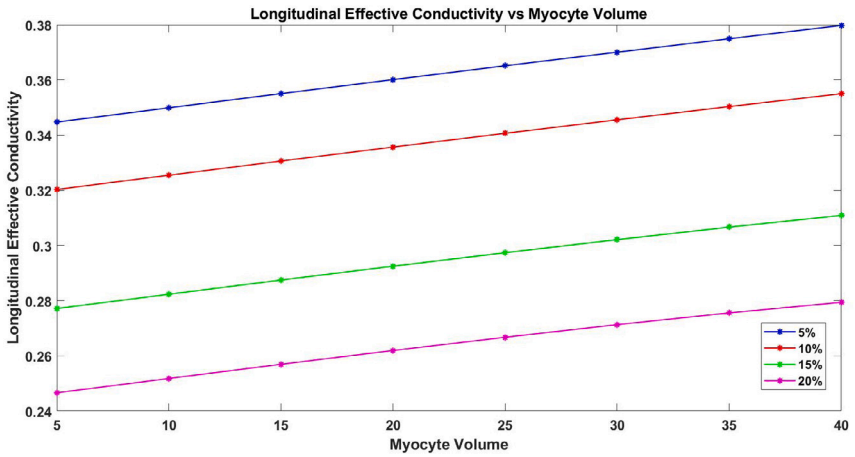

Fig. 5. The longitudinal conductance vs myocyte volume for four fixed fluid volume fractions.

6. Conclusions

In this work, we have derived a novel system of PDEs describing the effective electrical and mechanical behaviour of a vascularised poroelastic matrix with embedded electro-active inclusions (representing the myocytes) and a vascular network designed to represent the myocardium tissue.

Here we have applied the asymptotic homogenisation technique to a set of equations that we have developed to capture the behaviour of the mechanical and electrical deformations of the perfused myocardium. Due to the multiscale nature of the heart we can assume that the size of the heart muscle is much larger than the scale where we can identify individual elastic myocytes embedded in the poroelastic extracellular matrix with the permeating vasculature embedded in the matrix surrounding the myocytes. The scale where all these features are visible has been described as the microscale. This microscale has a length that is much smaller than the length of the entire heart muscle. If we zoom in further on the extracellular matrix then we find that the domain is a porous matrix with a fluid flow in the pores. We call this scale the porescale. To account for this porescale microstructure we use the governing equations of Biot's poroelasticity in the extracellular matrix. At the scale of the heart muscle, we can no longer visibly see any myocytes or permeating vasculature and therefore we call this the macroscale. Due to the sharp scale separation that this system possesses, we could rely on the asymptotic homogenisation technique to upscale the microstructural problem.

In doing so we account for the continuity of current densities, stresses, elastic displacements, and also the difference in the electric potentials and no flux on the interface between the elastic myocyte and the poroelastic matrix. Furthermore we account for the continuity of fluxes, stresses, fluid transport, slip over the porous surface, and the insulation of the current density on the interface between the vascular network and the poroelastic extracellular matrix.

The novel macroscale governing equations comprise a balance equation for the current densities and a balance equation for the stresses. These balance equations both contain terms that allow for the model to account for the difference in the electric potentials at different points in the microstructure as well as the differences in elastic properties of the underlying microstructure. We also have two further balance equations, one for the relative fluid–solid velocities of the vessels and one for the interstitial fluid. These equations also give information on how the strains of the elastic myocytes and the poroelastic extracellular matrix relate to the fluid transport between the compartments due to the leakage of the fluid from the vessels into the poroelastic matrix. Due to the model being derived via asymptotic homogenisation the coefficients in the governing equations allow for the properties of the microstructure to be retained. These coefficients are found by solving the microscale differential problems that we present which are different from the cell problems found in the works that precede this.

We should note that this work has extended the model for vascularised poroelastic materials (Penta and Merodio, 2017), the electrical and mechanical bidomain model (Miller and Penta, 2023) and the models of a poroelastic matrix with elastic inclusion (Royer et al., 2019; Chen et al., 2020). This work combines (Penta and Merodio, 2017; Miller and Penta, 2023) The amalgamation of all these works has allowed us to create a vascularised, electrical and mechanical myocardium model, where there is an even deeper underlying poroelastic structure encoded in the matrix. The combination of all these features across 3 physical scales of resolution is encoded in the final macroscale model which allows for a greater understanding of the myocardial behaviour due to the realistic microstructure that is considered.

The key novelty of the model is that it captures the electrical, mechanical and vascular behaviour of the myocardium. The differences in electrical properties are captured through the balance of current densities which comprise both the electric fields of each compartment premultiplied by second rank tensors that are to be obtained by solving the cell problems (44a)–(44e) and (45a)–(45e) and a vector term that arises from premultiplying the solutions to the cell problem (46a)–(46e) by the conductivity tensors. The mechanical deformations are captured via the balance of stresses which contains terms which are to be found by solving (63a)–(63e) that account for the varying elastic properties at different points in the microstructure. The stresses also contain terms relating to the interstitial pressure and the fluid pressure where the coefficients of these terms are to be found by solving (64a)–(64e) and (65a)–(65e). The balance Eq. (114b) also has terms that show the influence of the electric potentials and Lorentz forces on the deformations of the material. The balance of the relative fluid–solid velocities of the vessels and interstitial fluid capture the behaviour of the fluid network flow and the poroelastic flow. These equations describe the myocardium in terms of the strains of the elastic myocyte and the poroelastic extracellular matrix and the fluid transport between the compartments due to the leakage of the fluid from the vessels into the poroelastic matrix, where the coefficients are to be obtained by solving (80a)–(80d) and (103a)–(103c).

The new model has been developed to study the electrical and mechanical properties of the perfused myocardium and can be used to model both the healthy and diseased heart. Having a model that can describe the mechanical deformations, the perfusion and the electrical activity of

the myocardium is a very useful tool. The novel model can be used to understand how the electrical function and the elastic deformations can be impaired or changed by various diseases or disorders of the heart conduction system. With the novel model, we have derived here we can investigate how the structural changes caused by myocardial ischaemia induce differences in the heart electrophysiology.

The model presented in this work has some limitations that can well be addressed to give a more thorough understanding of the myocardium behaviour. In this work we have assumed that the myocytes and extracellular matrix undergo finite deformations (linear). This means that the extracellular matrix is described using Biot's standard poroelasticity and the myocytes are modelled using linear elasticity theory. We would however be able to extend this work by assuming that each phase is subject to large deformations and therefore use a nonlinear poroelastic formulation for the extracellular matrix, such as those presented in Brown et al. (2014), Collis et al. (2017) and Miller and Penta (2021b), and a nonlinear elastic formulation with a strain energy function chosen to capture the behaviour of the myocytes. These extensions do however cause a large increase in the computational complexity as we no longer have the full decoupling of scales. This leads to the cell problems having a very large computational expense to be solved. There are emerging techniques in the literature that are working to overcome this issue, such as in Dehghani and Zilian (2021, 2023) to make extensions of this kind much more computationally possible. This way, comparisons with alternative approaches such as those dealt with in Pezzuto et al. (2014) will also be possible.

We have that the difference in the electric potentials V is a given and that it depends only on the macroscale variable at leading order. As $V^{(0)}$, and also $V^{(1)}$ which is the term that drives the cell problem (41b)–(41e), are the differences in electrical potentials and arise because of transport of ions at a finer microstructural level than we are considering in this work, it would be possible to create a finer scale problem to obtain an expression for these values and cell problems from which they can be calculated. This would mean that we would be able to encode another further level of microstructural complexity in the model.

It would also be possible to incorporate further finer scale components of the microstructure such as collagen and elastin fibres in the matrix portion of our model. We could consider an approach such as taken in Federico and Herzog (2008) and Hashlamoun et al. (2016) which focus on the influence of microstructural fibre arrangements both in soft tissues and porous media. A further extension could be to consider a modification to the assumption that the blood vessels are insulated to the electrical activity. This would involve changing the interface conditions to allow for electrical current to flow into the vessels which could then be used to understand if the electrical activity provides enhancement to the perfusion.

This paper could be further developed to theoretically add transport of solute between the domains via delivery from the vessels such as to investigate drug delivery to the myocardium. This could be used to determine the effects of drug delivery on the treatment of heart diseases. We can study the use of nanoparticles to treat cardiovascular diseases such as in the studies (Fan et al., 2020; Suarez et al., 2015; Zhang et al., 2018). This can involve incorporating the flow of nanoparticles over a porous medium (Mahabaleshwar et al., 2023) and nanofluid flow due to stretching/shrinking porous materials (Vishalakshi et al., 2021) in our current framework. We could also consider a non-Newtonian fluid and the influence on mass transfer and the slip condition in porous media (Sneha et al., 2024).

CRediT authorship contribution statement

Laura Miller: Writing – review & editing, Writing – original draft, Visualization, Software, Project administration, Methodology, Investigation, Funding acquisition, Formal analysis, Conceptualization. **Raimondo Penta:** Writing – review & editing, Supervision, Project administration, Methodology, Investigation, Funding acquisition, Formal analysis, Conceptualization.

Declaration of competing interest

The authors declare that they have no known competing financial interests or personal relationships that could have appeared to influence the work reported in this paper.

Acknowledgments

LM is supported by EPSRC, United Kingdom, UK Grant EP/T517896/1. RP is partially supported by EPSRC, United Kingdom, UK Grants EP/S030875/1 and EP/T017899/1 and conducted the research according to the inspiring scientific principles of the national Italian mathematics association Indam ("Istituto nazionale di Alta Matematica") GNFM group.

Appendix. — solving the model

We now provide a step-by-step guide that can be followed to solve the macroscale model (114a)–(114e). We begin by explaining how to obtain the effective model coefficients. We then detail how these coefficients will be used when solving (114a)–(114e). The model coefficients encode the structural details such as geometry and properties of the elastic, poroelastic and fluid phases as well as the electrical properties of the solid phases. Due to the fact that the model is derived via assuming macroscopic uniformity of the material (see Remark 3.2) then the two scales (microscale and macroscale) are fully decoupled and the guide below can be used to solve the model. We solve the model as follows

1. The first step is to set the original material properties of the myocyte and the extracellular matrix at the microscale and the fluid in the vessels. We choose to make the assumption that each of the domains is isotropic. For the myocyte, since it is elastic, we require two independent elastic constants that can be the Poisson ratio and Young's modulus (or alternatively the Lamé constants). We could however not make this assumption and just provide the elasticity tensor for each phase. For the extracellular matrix, since it is poroelastic we require the effective elasticity tensors $\mathbb{C}_e$, the Biot's tensor $\hat{\boldsymbol{\alpha}}_e$, the Biot's modulus M and the hydraulic conductivities K_e. Since we assume that the extracellular matrix is isotropic we need to fix 5 parameters. These parameters are two independent elastic constants e.g. the Poisson ratio and Young's modulus (or alternatively the Lamé constants), hydraulic conductivity, Biot's coefficient and Biot's modulus. We also must fix the original electrical properties such as the conductivity tensors in each phase with up to 9 components and the potential drop V across the interface. The last property we need to fix is the magnetic field $\mathbf{B}$. We also determine the fluid viscosity.
2. We must determine the microscale geometry, this includes defining the specific geometry of a single periodic cell and the volume of each of the phases.

3. We now begin the process that allows us to determine the macroscale model coefficients. We begin by solving the problems that will allow us to determine the tensors and vectors that contribute to the coefficients in the electrical current densities. We have the problems (44a)–(44e), (45a)–(45e) and (46a)–(46e) in components where we note subscripts Γ and γ refer to the interface on which the normal relates to

$$\frac{\partial}{\partial y_\delta}\left((\mathsf{G}_i)_{\delta\kappa}\frac{\partial(\boldsymbol{\Phi}_i)_\alpha}{\partial y_\kappa}\right)+\frac{\partial(\mathsf{G}_i)_{\delta\alpha}}{\partial y_\delta}=0 \qquad \text{in} \quad \Omega_i, \tag{A.1a}$$

$$\frac{\partial}{\partial y_\delta}\left((\mathsf{G}_e)_{\delta\kappa}\frac{\partial(\hat{\boldsymbol{\Phi}}_e)_\alpha}{\partial y_\kappa}\right)=0 \qquad \text{in} \quad \Omega_e, \tag{A.1b}$$

$$(\boldsymbol{\Phi}_i)_\alpha=(\hat{\boldsymbol{\Phi}}_e)_\alpha \qquad \text{on} \quad \Gamma, \tag{A.1c}$$

$$\left((\mathsf{G}_i)_{\delta\kappa}\frac{\partial(\boldsymbol{\Phi}_i)_\alpha}{\partial y_\kappa}-(\mathsf{G}_e)_{\delta\kappa}\frac{\partial(\hat{\boldsymbol{\Phi}}_e)_\alpha}{\partial y_\kappa}\right)(n_\Gamma)_\delta=-(\mathsf{G}_i)_{\delta\alpha}(n_\Gamma)_\delta \qquad \text{on} \quad \Gamma, \tag{A.1d}$$

$$\left((\mathsf{G}_e)_{\delta\kappa}\frac{\partial(\hat{\boldsymbol{\Phi}}_e)_\alpha}{\partial y_\kappa}\right)(n_\gamma)_\delta=0 \qquad \text{on} \quad \gamma, \tag{A.1e}$$

and

$$\frac{\partial}{\partial y_\delta}\left((\mathsf{G}_i)_{\delta\kappa}\frac{\partial(\hat{\boldsymbol{\Phi}}_i)_\alpha}{\partial y_\kappa}\right)=0 \qquad \text{in} \quad \Omega_i, \tag{A.2a}$$

$$\frac{\partial}{\partial y_\delta}\left((\mathsf{G}_e)_{\delta\kappa}\frac{\partial(\boldsymbol{\Phi}_e)_\alpha}{\partial y_\kappa}\right)+\frac{\partial(\mathsf{G}_e)_{\delta\alpha}}{\partial y_\delta}=0 \qquad \text{in} \quad \Omega_e, \tag{A.2b}$$

$$(\hat{\boldsymbol{\Phi}}_i)_\alpha=(\boldsymbol{\Phi}_e)_\alpha \qquad \text{on} \quad \Gamma, \tag{A.2c}$$

$$\left((\mathsf{G}_i)_{\delta\kappa}\frac{\partial(\hat{\boldsymbol{\Phi}}_i)_\alpha}{\partial y_\kappa}-(\mathsf{G}_e)_{\delta\kappa}\frac{\partial(\boldsymbol{\Phi}_e)_\alpha}{\partial y_\kappa}\right)(n_\Gamma)_\delta=(\mathsf{G}_e)_{\delta\alpha}(n_\Gamma)_\delta \qquad \text{on} \quad \Gamma, \tag{A.2d}$$

$$\left((\mathsf{G}_e)_{\delta\kappa}\frac{\partial(\boldsymbol{\Phi}_e)_\alpha}{\partial y_\kappa}\right)(n_\gamma)_\delta=(\mathsf{G}_e)_{\delta\alpha}(n_\gamma)_\delta \qquad \text{on} \quad \gamma, \tag{A.2e}$$

and

$$\frac{\partial}{\partial y_\alpha}\left((\mathsf{G}_i)_{\alpha\delta}\frac{\partial(\tilde{\phi}_i)}{\partial y_\delta}\right)=0 \qquad \text{in} \quad \Omega_i, \tag{A.3a}$$

$$\frac{\partial}{\partial y_\alpha}\left((\mathsf{G}_e)_{\alpha\delta}\frac{\partial(\tilde{\phi}_e)}{\partial y_\delta}\right)=0 \qquad \text{in} \quad \Omega_e, \tag{A.3b}$$

$$(\tilde{\phi}_i)-(\tilde{\phi}_e)=V^{(1)} \qquad \text{on} \quad \Gamma, \tag{A.3c}$$

$$\left((\mathsf{G}_i)_{\alpha\delta}\frac{\partial(\tilde{\phi}_i)}{\partial y_\delta}\right)(n_\Gamma)_\alpha=\left((\mathsf{G}_e)_{\alpha\delta}\frac{\partial(\tilde{\phi}_e)}{\partial y_\delta}\right)(n_\Gamma)_\alpha \qquad \text{on} \quad \Gamma, \tag{A.3d}$$

$$\left((\mathsf{G}_e)_{\alpha\delta}\frac{\partial(\tilde{\phi}_e)}{\partial y_\delta}\right)(n_\gamma)_\alpha=0 \qquad \text{on} \quad \gamma, \tag{A.3e}$$

The problems (A.1a)–(A.1e) and (A.2a)–(A.2e) are vector problems. These have driving forces of conductivity tensor of each phase applied to the normal of the interface. The problem (A.3a)–(A.3e) is a scalar problem.

4. We will now consider the elastic coefficients. We are able to solve the elastic-type cell problem (63a)–(63e) which has the solution auxiliary tensors $\mathbb{M}_e$ and $\mathbb{M}_i$. These tensors then appear in the macroscale model coefficients, such as in the leading order stress. The cell problem to be solved is, in components

$$\frac{\partial}{\partial y_\delta}\left((C_i)_{\alpha\delta\tau\kappa}\xi^{\eta\nu}_{\tau\kappa}(\mathcal{A}_i)\right)+\frac{\partial(C_i)_{\alpha\delta\eta\nu}}{\partial y_\delta}=0 \qquad \text{in} \quad \Omega_i, \tag{A.4a}$$

$$\frac{\partial}{\partial y_\delta}\left((C_e)_{\alpha\delta\tau\kappa}\xi^{\eta\nu}_{\tau\kappa}(\mathcal{A}_e)\right)+\frac{\partial(C_e)_{\alpha\delta\eta\nu}}{\partial y_\delta}=0 \qquad \text{in} \quad \Omega_e, \tag{A.4b}$$

$$(\mathcal{A}_i)_{\alpha\eta\nu}=(\mathcal{A}_e)_{\alpha\eta\nu} \qquad \text{on} \quad \Gamma, \tag{A.4c}$$

$$\left((C_i)_{\alpha\delta\tau\kappa}\xi^{\eta\nu}_{\tau\kappa}(\mathcal{A}_i)-(C_e)_{\alpha\delta\tau\kappa}\xi^{\eta\nu}_{\tau\kappa}(\mathcal{A}_e)\right)(n_\Gamma)_\delta=(C_e-C_i)_{\alpha\delta\eta\nu}(n_\Gamma)_\delta \qquad \text{on} \quad \Gamma \tag{A.4d}$$

$$(C_e)_{\alpha\delta\tau\kappa}\xi^{\eta\nu}_{\tau\kappa}(\mathcal{A}_e)(n_\gamma)_\delta=-(C_e)_{\alpha\delta\eta\nu}(n_\gamma)_\delta \qquad \text{on} \quad \gamma. \tag{A.4e}$$

The solution to problem (A.4a)–(A.4e) is found by fixing the couple of indices $\tau,\kappa=1,2,3$ such that we are solving six elastic-type cell problems. When we do this we obtain the strains $\xi^{\eta\nu}_{\tau\kappa}(\mathcal{A}_i)$ and $\xi^{\eta\nu}_{\tau\kappa}(\mathcal{A}_e)$ so that for each fixed couple of indices τ, κ we have a linear elastic problem. For other examples of where this process has been carried out and utilised see also [27, 11, 10]. We have used the notation

$$\begin{aligned}\xi^{\eta\nu}_{\tau\kappa}(\mathcal{A}_i)&=\frac{1}{2}\left(\frac{\partial(\mathcal{A}_i)_{\tau\eta\nu}}{\partial y_\kappa}+\frac{\partial(\mathcal{A}_i)_{\kappa\eta\nu}}{\partial y_\tau}\right);\\ \xi^{\eta\nu}_{\tau\kappa}(\mathcal{A}_e)&=\frac{1}{2}\left(\frac{\partial(\mathcal{A}_e)_{\tau\eta\nu}}{\partial y_\kappa}+\frac{\partial(\mathcal{A}_e)_{\kappa\eta\nu}}{\partial y_\tau}\right).\end{aligned} \tag{A.5}$$

We also have two more elastic-type cell problems (64a)–(64e) and (65a)–(65e) driven by variations in the constituents' compressibility since we have a poroelastic extracellular matrix and an elastic myocyte

$$\frac{\partial}{\partial y_\delta}\left((C_i)_{\alpha\delta\tau\kappa}\xi_{\tau\kappa}(a_i)\right)=0 \qquad \text{in} \quad \Omega_i, \tag{A.6a}$$

$$\frac{\partial}{\partial y_\delta}\left((C_e)_{\alpha\delta\tau\kappa}\xi_{\tau\kappa}(a_e)\right)=\frac{\partial(\hat{\alpha}_e)_{\alpha\delta}}{\partial y_\delta} \qquad \text{in} \quad \Omega_e, \tag{A.6b}$$

$$(a_i)_\alpha = (a_e)_\alpha \qquad \text{on} \qquad \Gamma, \tag{A.6c}$$

$$\big((C_i)_{\alpha\delta\tau\kappa}\xi_{\tau\kappa}(a_i) - (C_e)_{\alpha\delta\tau\kappa}\xi_{\tau\kappa}(a_e)\big)(n_\Gamma)_\delta = (\hat{\alpha}_e)_{\alpha\delta}(n_\Gamma)_\delta \qquad \text{on} \qquad \Gamma, \tag{A.6d}$$

$$((C_e)_{\alpha\delta\tau\kappa}\xi_{\tau\kappa}(a_e))(n_\gamma)_\delta = (\hat{\alpha}_e)_{\alpha\delta}(n_\gamma)_\delta - (n_\gamma)_\alpha \qquad \text{on} \qquad \gamma, \tag{A.6e}$$

and

$$\frac{\partial}{\partial y_\delta}\big((C_i)_{\alpha\delta\tau\kappa}\xi_{\tau\kappa}(b_i)\big) = 0 \qquad \text{in} \qquad \Omega_i, \tag{A.7a}$$

$$\frac{\partial}{\partial y_\delta}\big((C_e)_{\alpha\delta\tau\kappa}\xi_{\tau\kappa}(b_e)\big) = 0 \qquad \text{in} \qquad \Omega_e, \tag{A.7b}$$

$$(b_i)_\alpha = (b_e)_\alpha \qquad \text{on} \qquad \Gamma, \tag{A.7c}$$

$$\big((C_i)_{\alpha\delta\tau\kappa}\xi_{\tau\kappa}(b_i) - (C_e)_{\alpha\delta\tau\kappa}\xi_{\tau\kappa}(b_e)\big)(n_\Gamma)_\delta = 0 \qquad \text{on} \qquad \Gamma, \tag{A.7d}$$

$$\big((C_e)_{\alpha\delta\tau\kappa}\xi_{\tau\kappa}(a_e)\big)(n_\gamma)_\delta = -(n_\gamma)_\alpha \qquad \text{on} \qquad \gamma, \tag{A.7e}$$

where we have used the notation

$$\xi_{\tau\kappa}(\bullet) = \frac{1}{2}\left(\frac{\partial(\bullet)_\tau}{\partial y_\kappa} + \frac{\partial(\bullet)_\kappa}{\partial y_\tau}\right), \tag{A.8}$$

where $\bullet = a_i, a_e, b_i, b_e$. The solutions to problems (A.6a)–(A.6e) and (A.7a)–(A.7e) is obtained by solving 3 cell problems for each $\alpha = 1, 2, 3$.

5. We also have the cell problem (80a)–(80d) which we require to solve to find the coefficient of the Darcy equation governing fluid network flow. We have the cell problem in components

$$\frac{\partial(W_{\mathrm{f}})_{\delta\alpha}}{\partial y_\kappa \partial y_\kappa} - \frac{\partial(P_{\mathrm{f}})_\alpha}{\partial y_\delta} + \delta_{\alpha\delta} = 0 \qquad \text{in} \quad \Omega_{\mathrm{f}}, \tag{A.9a}$$

$$\frac{\partial(W_{\mathrm{f}})_{\alpha\delta}}{\partial y_\alpha} = 0 \qquad \text{in} \quad \Omega_{\mathrm{f}}, \tag{A.9b}$$

$$(W_{\mathrm{f}})_{\delta\alpha}(n_\gamma)_\delta = 0 \qquad \text{on} \quad \gamma, \tag{A.9c}$$

$$(\tau_\beta)_\delta \cdot \left(\frac{\partial(\mathsf{W}_{\mathrm{f}})_{\delta\alpha}}{\partial y_\kappa} + \frac{\partial(\mathsf{W}_{\mathrm{f}})_{\kappa\alpha}}{\partial y_\delta}\right)(n_\gamma)_\kappa = -\frac{\alpha}{\sqrt{k}}(\mathsf{W}_{\mathrm{f}})_{\delta\alpha} \cdot (\tau_\beta)_\delta \qquad \text{on} \quad \gamma, \tag{A.9d}$$

6. The last cell problems we require to solve give us the coefficients of the interstitial flow equation. We solve the problem (103a)–(103c). In components these are

$$\frac{\partial}{\partial y_\delta}\left((K_e)_{\delta\kappa}\frac{\partial(P_p)_\alpha}{\partial y_\kappa}\right) = -\frac{\partial(K_e)_{\delta\alpha}}{\partial y_\delta} \qquad \text{in} \quad \Omega_e \tag{A.10a}$$

$$\left((K_e)_{\delta\kappa}\frac{\partial(P_p)_\alpha}{\partial y_\kappa}\right)(n_\gamma)_\delta = -(K_e)_{\delta\alpha}(n_\gamma)_\delta \qquad \text{on} \quad \gamma \tag{A.10b}$$

$$\left((K_e)_{\delta\kappa}\frac{\partial(P_p)_\alpha}{\partial y_\kappa}\right)(n_\Gamma)_\delta = -(K_e)_{\delta\alpha}(n_\Gamma)_\delta \qquad \text{on} \quad \Gamma \tag{A.10c}$$

7. When solving the cell problems we need the solution to be unique. We therefore require one additional condition. We make the choice that the cell averages of the auxiliary variables are zero.
8. The auxiliary second rank tensors and vectors arising from the cell problems (Q_e, Q_i, R_e, R_i, L_i, L_e, N_i, N_e, W_{f}, $\nabla_{\mathbf{y}}\mathbf{P}_p$, $\mathbf{s}_e$ and $\mathbf{s}_i$) are then substituted in where they appear in the macroscale equations and this leads to a macroscale model with coefficients that encode the microstructural details.
9. The structure and geometry of the macroscale must be set. This includes giving boundary conditions for the homogenised cell. We also must provide initial conditions for the macroscale solid elastic displacement, pressure and the electric potential drop V.
10. Finally, after carrying out all the above steps our macroscale model (114a)–(114e) can then be solved.

Data availability

No data was used for the research described in the article.

References

Anversa, P., Beghi, C., Kikkawa, Y., Olivetti, G., 1985. Myocardial response to infarction in the rat. Morphometric measurement of infarct size and myocyte cellular hypertrophy. Am. J. Pathol. 118 (3), 484–492.

Bader, F., Bendahmane, M., Saad, M., Talhouk, R., 2021. Three scale unfolding homogenization method applied to cardiac bidomain model. Acta Appl. Math. 176 (14).

Bakhvalov, N.S., Panasenko, G., 2012. Homogenisation: Averaging Processes in Periodic Media: Mathematical Problems in the Mechanics of Composite Materials, vol. 36, Springer Science & Business Media.

Biot, M.A., 1955. Theory of elasticity and consolidation for a porous anisotropic solid. J. Appl. Phys. 26 (2), 182–185.

Biot, M.A., 1956a. General solutions of the equations of elasticity and consolidation for a porous material. J. Appl. Mech. 23 (1), 91–96.

Biot, M.A., 1956b. Theory of propagation of elastic waves in a fluid-saturated porous solid. II. Higher frequency range. J. Acoust. Soc. Am. 28 (2), 179–191.

Biot, M.A., 1962. Mechanics of deformation and acoustic propagation in porous media. J. Appl. Phys. 33 (4), 1482–1498.

Brown, D.L., Popov, P., Efendiev, Y., 2014. Effective equations for fluid-structure interaction with applications to poroelasticity. Appl. Anal. 93 (4), 771–790.

Burridge, R., Keller, J.B., 1981. Poroelasticity equations derived from microstructure. J. Acoust. Soc. Am. 70 (4), 1140–1146.

Chen, M., Kimpton, L., Whiteley, J., Castilho, M., Malda, J., Please, C., Waters, S., Byrne, H., 2020. Multiscale modelling and homogenisation of fibre-reinforced hydrogels for tissue engineering. Eur. J. Appl. Math. 31 (1), 143–171.

Cioranescu, D., Donato, P., 1999. An Introduction to Homogenization, vol. 17, Oxford University Press.
Collis, J., Brown, D., Hubbard, M.E., O'Dea, R.D., 2017. Effective equations governing an active poroelastic medium. Proc. R. Soc. A 473 (2198), 20160755.
Cookson, A., Lee, J., Michler, C., Chabiniok, R., Hyde, E., Nordsletten, D., Sinclair, M., Siebes, M., Smith, N., 2012. A novel porous mechanical framework for modelling the interaction between coronary perfusion and myocardial mechanics. J. Biomech. 45 (5), 850–855.
Dalwadi, M.P., Griffiths, I.M., Bruna, M., 2015. Understanding how porosity gradients can make a better filter using homogenization theory. Proc. R. Soc. A 471 (2182).
Davit, Y., Bell, C.G., Byrne, H.M., Chapman, L.A., Kimpton, L.S., Lang, G.E., Leonard, K.H., Oliver, J.M., Pearson, N.C., Shipley, R.J., 2013. Homogenization via formal multiscale asymptoticsand volume averaging:how do the two techniques compare? Adv. Water Resour. 62, 178–206.
Dehghani, H., Penta, R., Merodio, J., 2018. The role of porosity and solid matrix compressibility on the mechanical behavior of poroelastic tissues. Mater. Res. Express 6 (3), 035404.
Dehghani, H., Zilian, A., 2021. ANN-aided incremental multiscale-remodelling-based finite strain poroelasticity. Comput. Mech. 68 (1), 131–154.
Dehghani, H., Zilian, A., 2023. Finite strain poro-hyperelasticity: an asymptotic multi-scale ALE-FSI approach supported by ANNs. Comput. Mech. 1–25.
Di Gregorio, S., Fedele, M., Pontone, G., Corno, A.F., Zunino, P., Vergara, C., Quarteroni, A., 2021. A computational model applied to myocardial perfusion in the human heart: from large coronaries to microvasculature. J. Comput. Phys. 424, 109836.
Di Stefano, S., Miller, L., Grillo, A., Penta, R., 2020. Effective balance equations for electrostrictive composites. Z. Angew. Math. Phys. 71 (166).
Dorfmann, L., Ogden, R., 2006. Nonlinear electroelastic deformations. J. Elasticity 82, 99–127.
Dorfmann, L., Ogden, R.W., 2014. Nonlinear Theory of Electroelastic and Magnetoelastic Interactions, vol. 1, Springer.
Fan, C., Joshi, J., Li, F., Xu, B., Khan, M., Yang, J., Zhu, W., 2020. Nanoparticle-mediated drug delivery for treatment of ischemic heart disease. Front. Bioeng. Biotechnol. 8, 687.
Federico, S., Herzog, W., 2008. On the permeability of fibre-reinforced porous materials. Int. J. Solids Struct. 45 (7–8), 2160–2172.
Fu, Y., 2024. Elastic localizations. In: Electro-and Magneto-Mechanics of Soft Solids: Constitutive Modelling, Numerical Implementations, and Instabilities. Springer, pp. 141–177.
Hashlamoun, K., Grillo, A., Federico, S., 2016. Efficient evaluation of the material response of tissues reinforced by statistically oriented fibres. Z. Angew. Math. Phys. 67, 1–32.
Holmes, M.H., 2012. Introduction to Perturbation Methods, vol. 20, Springer Science & Business Media, New York.
Holzapfel, G.A., Ogden, R.W., 2009. Constitutive modelling of passive myocardium: a structurally based framework for material characterization. Phil. Trans. R. Soc. A 367 (1902), 3445–3475.
Hori, M., Nemat-Nasser, S., 1999. On two micromechanics theories for determining micro-macro relations in heterogeneous solid. Mech. Mater. 31, 667–682.
Katz, A.M., 2010. Physiology of the Heart. Lippincott Williams & Wilkins.
Liguori, P., Gei, M., 2023. New actuation modes of composite dielectric elastomers. Proc. R. Soc. A 479 (2275), 20230168.
Mahabaleshwar, U., Anusha, T., Hatami, M., 2023. Analysis of a stagnation point flow with hybrid nanoparticles over a porous medium. Fluid Dynam. Mater. Process. 19 (2).
Mascheroni, P., Penta, R., Merodio, J., 2023. The impact of vascular volume fraction and compressibility of the interstitial matrix on vascularised poroelastic tissues. Biomech. Model. Mechanobiol. 22 (6), 1901–1917.
Maugin, G.A., 2013. Continuum Mechanics of Electromagnetic Solids. Elsevier.
Miller, L., Penta, R., 2020. Effective balance equations for poroelastic composites. Contin. Mech. Thermodyn. 32 (6), 1533–1557.
Miller, L., Penta, R., 2021a. Double poroelasticity derived from the microstructure. Acta Mech. 232, 3801–3823.
Miller, L., Penta, R., 2021b. Homogenized balance equations for nonlinear poroelastic composites. Appl. Sci. 11 (14), 6611.
Miller, L., Penta, R., 2022a. Investigating the effects of microstructural changes induced by myocardial infarction on the elastic parameters of the heart. Biomech. Model. Mechanobiol..
Miller, L., Penta, R., 2022b. Micromechanical analysis of the effective stiffness of poroelastic composites. Eur. J. Mech. / A Solids 98, 104875.
Miller, L., Penta, R., 2023. Homogenization of a coupled electrical and mechanical bidomain model for the myocardium. Math. Mech. Solids 10812865231207600.
Ng, E., Ghista, D., Jegathese, R., 2005. Perfusion studies of steady flow in poroelastic myocardium tissue. Comput. Methods Biomech. Biomed. Eng. 8 (6), 349–357.
Olivetti, G., Melissari, M., Balbi, T., Quaini, F., Cigola, E., Sonnenblick, E., Anversa, P., 1994. Myocyte cellular hypertrophy is responsible for ventricular remodelling in the hypertrophied heart of middle aged individuals in the absence of cardiac failure. Cardiovasc. Res. 28 (8), 1199–1208.
Olivetti, G., Ricci, R., Beghi, C., Guideri, G., Anversa, P., 1987. Response of the borderzone myocardial infarction in rats. Am. J. Pathol. 125, 476–483.
Opie, L.H., 2004. Heart Physiology: from Cell to Circulation. Lippincott Williams & Wilkins.
Owen, B., Bojdo, N., Jivkov, A., Keavney, B., Revell, A., 2018. Structural modelling of the cardiovascular system. Biomech. Model. Mechanobiol. 17 (5), 1217–1242.
Parnell, W.J., Abrahams, I.D., 2006. Dynamic homogenization in periodic fibre reinforced media. Quasi-static limit for SH waves. Wave Motion 43 (6), 474–498.
Parnell, W., Abrahams, I., 2008. Homogenization for wave propagation in periodic fibre-reinforced media with complex microstructure. I—theory. J. Mech. Phys. Solids 56 (7), 2521–2540.
Peirlinck, M., Costabal, F., Yao, J., Guccione, J., Tripathy, S., Wang, Y., Ozturk, D., Segars, P., Morrison, T., Levine, S., Kuhl, E., 2021. Precision medicine in human heart modeling: Perspectives, challenges, and opportunities. Biomech. Model. Mechanobiol. 20, 803–831.
Penta, R., Ambrosi, D., Shipley, R.J., 2014. Effective governing equations for poroelastic growing media. Q. J. Mech. Appl. Math. 67 (1), 69–91.
Penta, R., Gerisch, A., 2015. Investigation of the potential of asymptotic homogenization for elastic composites via a three-dimensional computational study. Comput. Vis. Sci. 17 (4), 185–201.
Penta, R., Gerisch, A., 2017a. The asymptotic homogenization elasticity tensor properties for composites with material discontinuities. Contin. Mech. Thermodyn. 29, 187–206.
Penta, R., Gerisch, A., 2017b. An introduction to asymptotic homogenization. In: Multiscale Models in Mechano and Tumor Biology. Springer, pp. 1–26.
Penta, R., Merodio, J., 2017. Homogenized modeling for vascularized poroelastic materials. Meccanica 52 (14), 3321–3343.
Penta, R., Miller, L., Grillo, A., Ramírez-Torres, A., Mascheroni, P., Rodríguez-Ramos, R., 2020. Porosity and diffusion in biological tissues. Recent advances and further perspectives. In: Constitutive Modelling of Solid Continua. Springer, pp. 311–356.
Penta, R., Ramirez Torres, A., Merodio, J., Rodriguez-Ramos, R., 2018. Effective balance equations for elastic composites subject to inhomogeneous potentials. Contin. Mech. Thermodyn. 30, 145–163.
Penta, R., Ramirez Torres, A., Merodio, J., Rodriguez-Ramos, R., 2021. Effective governing equations for heterogenous porous media subject to inhomogeneous body forces. Math. Eng. 3 (4), 1–17.
Pesavento, F., Schrefler, B.A., Sciumè, G., 2017. Multiphase flow in deforming porous media: A review. Arch. Comput. Methods Eng. 24, 423–448.
Pezzuto, S., Ambrosi, D., Quarteroni, A., 2014. An orthotropic active–strain model for the myocardium mechanics and its numerical approximation. Eur. J. Mech. A Solids 48, 83–96.
Purslow, P., 2008. The extracellular matrix of skeletal and cardiac muscle. In: Collagen: Structure and Mechanics. Springer US, pp. 325–357.
Puwal, S., Roth, B.J., 2010. Mechanical bidomain model of cardiac tissue. Phys. Rev. E 82, 041904.
Richardson, G., Chapman, S.J., 2011. Derivation of the bidomain equations for a beating heart with a general microstructure. SIAM J. Appl. Math. 71 (3), 657–675.
Rohan, E., Cimrman, R., 2010. Two-scale modeling of tissue perfusion problem using homogenization of dual porous media. Int. J. Multiscale Comput. Eng. 8 (1).
Rohan, E., Naili, S., Cimrman, R., Lemaire, T., 2012. Multiscale modeling of a fluid saturated medium with double porosity: Relevance to the compact bone. J. Mech. Phys. Solids 60 (5), 857–881.
Rohan, E., Naili, S., Lemaire, T., 2016. Double porosity in fluid-saturated elastic media: deriving effective parameters by hierarchical homogenization of static problem. Contin. Mech. Thermodyn. 28, 1263–1293.
Rohan, E., Turjanicová, J., Lukeš, V., 2021. Multiscale modelling and simulations of tissue perfusion using the Biot-Darcy-Brinkman model. Comput. Struct. 251, 106404.
Roth, B.J., 1991. Action potential propagation in a thick strand of cardiac muscle. Circ. Res. 68 (1), 162–173.
Roth, B.J., 1992. How the anisotropy of the intracellular and extracellular conductivities influences stimulation of cardiac muscle. J. Math. Biol. 30, 633–646.
Roth, B.J., 2016. A mathematical model of mechanotransduction. Acad. Biol.
Royer, P., Recho, P., Verdier, C., 2019. On the quasi-static effective behaviour of poroelastic media containing elastic inclusions. Mech. Res. Commun. 96, 19–23.
Sachse, F.B., Moreno, A., Seemann, G., Abildskov, J., 2009. A model of electrical conduction in cardiac tissue including fibroblasts. Ann. Biomed. Eng. 37, 874–889.
Sanchez-Palencia, E., 2006. Homogenization method for the study of composite media. In: Asymptotic Analysis II— Surveys and New Trends. Springer, pp. 192–214.
Smith, N., Nickerson, D., Crampin, E., Hunter, P., 2004. Multiscale computational modelling of the heart. Acta Numer. 13, 371–431.
Sneha, K., Mahesh, R., Mahabaleshwar, U., Souayeh, B., 2024. A non-Newtonian fluid flow due to porous media with mass transfer and slip. Internat. J. Modern Phys. B 38 (09), 2450130.

Suarez, S., Almutairi, A., Christman, K., 2015. Micro-and nanoparticles for treating cardiovascular disease. Biomater. Sci. 3 (4), 564–580.
Vishalakshi, A., Mahabaleshwar, U., Bhattacharayya, S., 2021. Study of mixed convective nanofluid flow due to porous stretching/shrinking sheet with heat transfer. In: Conference on Fluid Mechanics and Fluid Power. Springer, pp. 179–184.
Weidmann, S., 1974. Heart: electrophysiology. Annu. Rev. Physiol. 36 (1), 155–169.
Weinhaus, A.J., Roberts, K.P., 2005. Anatomy of the human heart. In: Handbook of Cardiac Anatomy, Physiology, and Devices. Humana Press, pp. 51–79.
Whitaker, R.H., 2014. The normal heart: Anatomy of the heart. Medicine 42 (8), 406–408.
Zhang, J., Ma, A., Shang, L., 2018. Conjugating existing clinical drugs with gold nanoparticles for better treatment of heart diseases. Front. Physiol. 9, 642.